Discovery of Selective and Potent Inhibitors of Gram-Positive Bacterial Thymidylate Kinase (TMK)

Gabriel Martínez-Botella,*,[†,||] John N. Breen,[†,‡] James E. S. Duffy,[§] Jacques Dumas,[†] Bolin Geng,[†] Ian K. Gowers,[§] Oluyinka M. Green,[†] Satenig Guler,[†] Martin F. Hentemann,[†] Felix A. Hernandez-Juan,[§] Diane Joseph-McCarthy,[†] Sameer Kawatkar,[†] Nicholas A. Larsen,[‡] Ovadia Lazari,[§] James T. Loch,[†] Jacqueline A. Macritchie,[§] Andrew R. McKenzie,[†] Joseph V. Newman,[†] Nelson B. Olivier,[‡] Linda G. Otterson,[†] Andrew P. Owens,[§] Jon Read,[‡] David W. Sheppard,[§] and Thomas A. Keating[†]
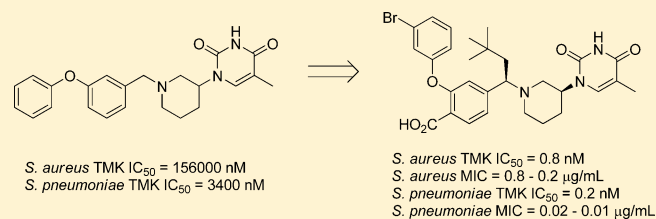
[†]AstraZeneca Infection Innovative Medicines, 35 Gatehouse Drive, Waltham, Massachusetts 02451, United States
[‡]AstraZeneca Discovery Sciences, 35 Gatehouse Drive, Waltham, Massachusetts 02451, United States
[§]BioFocus, Chesterford Research Park, Saffron Walden CB10 1XL, U.K.

Ⓢ *Supporting Information*

ABSTRACT: Thymidylate kinase (TMK) is an essential enzyme in bacterial DNA synthesis. The deoxythymidine monophosphate (dTMP) substrate binding pocket was targeted in a rational-design, structure-supported effort, yielding a unique series of antibacterial agents showing a novel, induced-fit binding mode. Lead optimization, aided by X-ray crystallography, led to picomolar inhibitors of both *Streptococcus pneumoniae* and *Staphylococcus aureus* TMK. MICs < 1 µg/mL were achieved against methicillin-resistant *S. aureus* (MRSA), *S. pneumoniae*, and vancomycin-resistant *Enterococcus* (VRE). Log *D* adjustments yielded single diastereomers 14 (TK-666) and 46, showing a broad antibacterial spectrum against Gram-positive bacteria and excellent selectivity against the human thymidylate kinase ortholog.

S. aureus TMK IC$_{50}$ = 156000 nM
S. pneumoniae TMK IC$_{50}$ = 3400 nM

S. aureus TMK IC$_{50}$ = 0.8 nM
S. aureus MIC = 0.8 - 0.2 µg/mL
S. pneumoniae TMK IC$_{50}$ = 0.2 nM
S. pneumoniae MIC = 0.02 - 0.01 µg/mL

■ INTRODUCTION

The discovery of novel antibacterial classes has proven particularly challenging for the research community in both industry and academia in the last few decades.[1] The onset of the genomic era and the promise of the discovery of novel mechanisms have not translated into marketed drugs.[2] The need for new antibiotics to treat drug-resistant Gram-positive infections is acute, especially against methicillin-resistant *Staphylococcus aureus* and *Staphylococcus epidermidis* and vancomycin-resistant *Enterococcus faecium* and *Enterococcus faecalis*.[3] In this context, structure-guided design approaches[4] have yielded some initial success in addressing the resistance of existing classes, for example the drug candidate Iclaprim,[5] and novel chemical classes of DNA gyrase inhibitors.[6] We have recently reported the first *in vivo* efficacious inhibitor of thymidylate kinase (TMK) targeting Gram-positive bacteria.[7] TMK is a nucleotide kinase that catalyzes the phosphorylation of deoxythymidine monophosphate (dTMP) to deoxythymidine diphosphate (dTDP) using ATP as a cosubstrate. This is a necessary step in the biosynthesis of deoxythymidine triphosphate (dTTP) for DNA synthesis. While dTMP can be produced both *de novo* (from dUMP) and *via* salvage (from thymidine), neither it nor dTDP can be imported into the cell nor biosynthesized through an alternate path. This makes TMK an essential enzyme and a very attractive target for therapeutic intervention.[8] This report describes the discovery of the first high-quality inhibitors of Gram-positive bacterial TMK employing a structure-guided approach.

■ CHEMISTRY

Piperidinylthymine analogs were synthesized as described in Schemes 1, 2, and 3. The key intermediate, piperidinylthymine 1, was prepared using commercially available racemic- or (R)- or (S)-*tert*-butyl 3-aminopiperidine-1-carboxylate (3) and 3-methoxyacrylic acid (2) (Scheme 1). Standard reductive amination conditions to couple 1 with benzaldehydes afforded the analogs described in Tables 1 and 2. Scheme 2 shows the synthesis for compounds in Table 3. 2-Fluoro-4-formylbenzonitrile (5) and 1 afforded intermediate 6 under reductive amination conditions using polymer-supported cyanoborohydride. The addition of phenols, followed by the hydrolysis of the cyano group in 7 gave the desired compounds in moderate yields. In order to install an aliphatic side chain in the benzylic carbon bridging the piperidine and the central phenyl ring, addition of commercially available zincate 9 to acid chlorides was performed routinely and in high yields (Scheme 3). The resulting ketone 11a was transformed into mesylate 11b and then coupled to 1 in moderate yields, though, in some instances, this reaction led to elimination products. The ketone
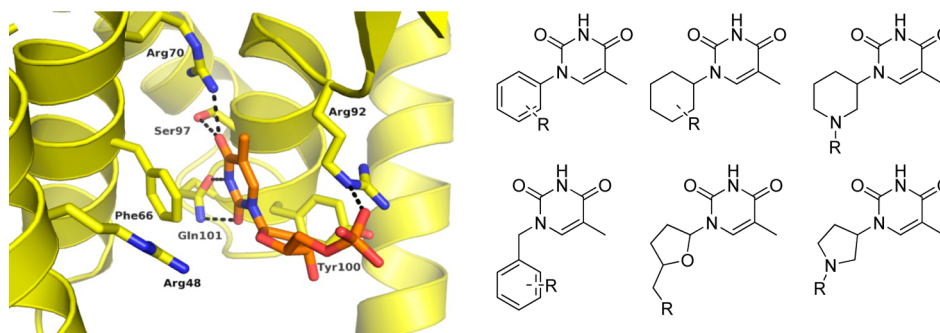
Figure 1. The crystal structure of the *Staphylococcus aureus* thymidylate kinase (TMK) with bound dTMP (left)[9] was the starting point for design of lead inhibitor scaffolds (right). dTMP is depicted in orange, with the terminal phosphate located at the right-hand side of the panel. This phosphate points in the direction of the substrate channel leading to the ATP binding site (not shown).

11a and protected 3-aminopiperidine could alternately be coupled under standard reductive amination conditions and the thymine ring built as described in Scheme 1. Installation of the phenoxy ring was carried out under microwave conditions, followed by subsequent hydrolysis of the benzonitrile under aqueous basic conditions (Scheme 3). The diastereomeric mixture **13** was then separated, affording pure diastereomers (Scheme 3).
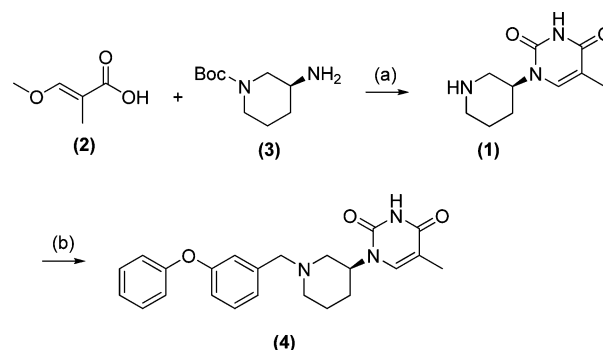
■ RESULTS AND DISCUSSION

The X-ray structure of dTMP bound to *S. aureus* TMK[9] provided the starting point for the rational design of thymine-containing scaffolds (Figure 1). A set of deoxyribose-replacement ring systems were designed from docking models, and small libraries of each scaffold were synthesized by coupling available R groups. These compounds were screened for inhibition against the *S. aureus* and *S. pneumoniae* TMK enzymes. While nearly all of the compounds synthesized were inactive, as a result of this effort, thymine-based racemic compound **15** was discovered (Figure 2). Compound **15** has
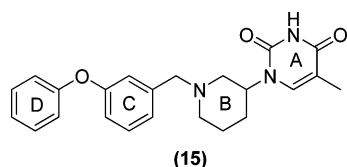
Figure 2. Structure of thymidylate kinase (TMK) racemic lead inhibitor **15**. The rings are lettered A–D for discussion in the text.

moderate affinity against *S. pneumoniae* TMK (IC$_{50}$ = 3.4 μM) and low affinity against *S. aureus* TMK (IC$_{50}$ = 156 μM), but given the dearth of other leads, it was pursued in a medicinal chemistry program. An early survey of the phenoxy ring (Table 1) led to racemic compound **16**, which was suitable for protein crystallography, yielding the first structure of an inhibitor bound to *S. aureus* and a distinct binding mode when compared to dTMP[7,9] (Figure 3). The X-ray structure showed the thymine ring (ring A) retaining its position from dTMP, and anchoring the inhibitor by creating multiple hydrogen bonds with residues Arg70, Ser97, and Gln101, and π-stacking with Phe66. Strikingly, a single enantiomer (*S*)-**16** was found in the crystal structure, which positions the compound to bend *away* from the substrate binding channel rather than following it as the dTMP substrate does. The piperidine (ring B) in this enantiomer provided the correct geometry to enable the turn. The middle phenyl ring (ring C) appeared to act as a spacer,

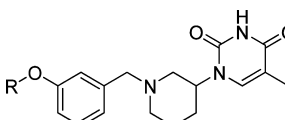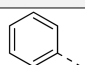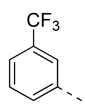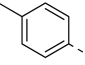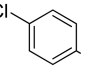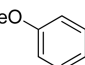## Scheme 1. Synthesis of TMK Inhibitors in Tables 1 and 2[a]

[a](a) (i) oxalyl chloride, AgOCN, 95 °C, 3 h; (ii) H$_2$SO$_4$, MeOH, 95 °C, 16 h, 40% overall; (b) 3-phenoxybenzaldehyde, trimethylammonium cyanoborohydride, 22 °C, 16 h, 19%.
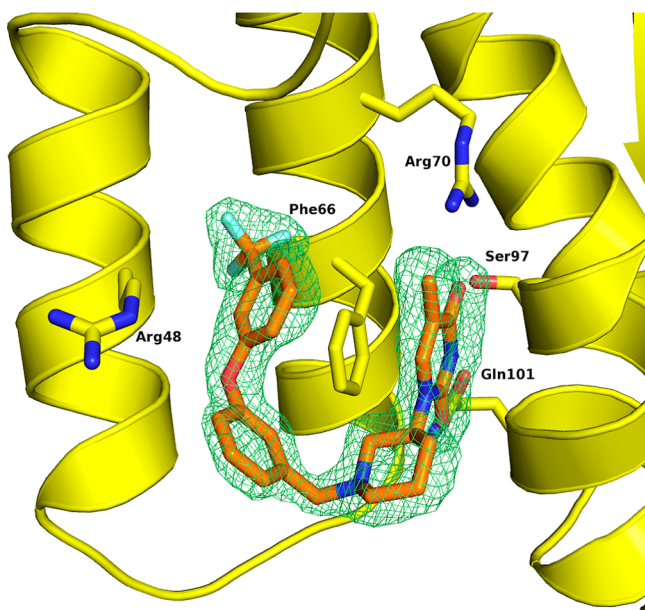
placing the phenoxy ring (ring D) into a newly revealed hydrophobic pocket, created by movement of a helix and a loop at the left-hand side of the binding pocket.[7] This pocket is not evident in the apo or dTMP structures.[9] To verify the insight gained from the crystal structure, several enantiomeric pairs (**27**−**30**) were synthesized (Table 2), starting with enantiomerically pure *tert*-butyl 3-aminopiperidine-1-carboxylate (**2**) (Scheme 1). In all cases, the (*S*)-enantiomer was 12- to 100-fold more potent against both *S. pneumoniae* and *S. aureus* TMK enzymes than the (*R*)-enantiomer.

With the X-ray structure of (*S*)-**16** in hand, binding was improved by first modifying ring D. Two approaches were employed: first, a virtual library of compounds with substituted phenoxy rings was docked into the binding pocket of *S. aureus* TMK.[10] Results suggested that a great variety of substitutions could be tolerated in this pocket. Based on this, a set of compounds were synthesized and tested. However, little improvement was observed in the activity compared to the case of **16**. Second, a more traditional Topliss method was also employed in parallel to the above-mentioned structure-based approach. The Topliss method[11] is based on the assumption that any substitution will modify the biological activity relative to the parent compound as a result of changes in hydrophobic, electronic, and steric effects. This approach resulted in compounds with significant improvements in enzyme inhibition. In particular, the 3-Cl and 3-Br analogs (**22**, **23**) achieved more than a 100-fold improvement against both *S. pneumoniae* TMK and *S. aureus* TMK. Such an improvement most likely resulted from a combination of desolvation and favorable

Table 1. TMK Inhibition Activity of Analogues of 15

Compound	R	*S. pneumoniae* IC$_{50}$ (nM)	*S. aureus* IC$_{50}$ (nM)
15	(phenyl)	3400	156000
16	(CF$_3$-phenyl)	15000	24000
17	(methyl-phenyl)	6000	59000
18	(Cl-phenyl)	1300	35000
19	(MeO-phenyl)	9000	143000

Figure 3. Crystal structure of (*S*)-**16** bound to *S. aureus* TMK at 2.0 Å. The green mesh represents the $2F_o − F_c$ electron density map contoured to 1 σ. Racemic **16** was soaked with protein crystals, but only the single enantiomer was found to be bound. Compared to the binding mode of dTMP (Figure 1), the position and contacts of thymine ring A are extremely well-conserved. However, piperidinyl ring B, instead of executing a turn toward the substrate channel (off right-hand side of panel) instead bends the molecule to the left, into a newly formed, induced-fit binding pocket for ring D. This pocket is not evident in the Figure 1 structure. Major changes in protein structure to create this cryptic pocket include rotation of the Arg48 side chain, movement of the α2 helix (leftmost in figure), and movement of the connecting loop at the top left of the figure. Phe66 forms a π-stack with rings A and D.
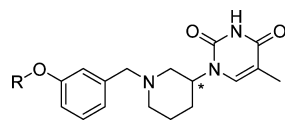
hydrophobic interactions. These inhibitors do, however, show a higher affinity, ∼10-fold, against *S. pneumoniae* TMK versus *S. aureus* TMK. The difference in compound potency between these two species may be attributed to the nature of the hydrogen bond network formed between protein and compound. The scaffold presented herein interacts with the binding site such that rings A and D form a π-stacking interaction with an aromatic residue: Tyr71 and Phe66 in *S. pneumoniae* and *S. aureus* TMK, respectively.[7] We hypothesize that the hydroxyl group of *S. pneumoniae* Tyr71 forms a hydrogen bond to the thymine carbonyl group. As the hydrogen bonding energy between two uncharged groups is estimated to be 0.5−1.8 kcal/mol,[12] we ascribe the roughly 10-fold difference in IC$_{50}$ between the orthologs to the additional interaction.
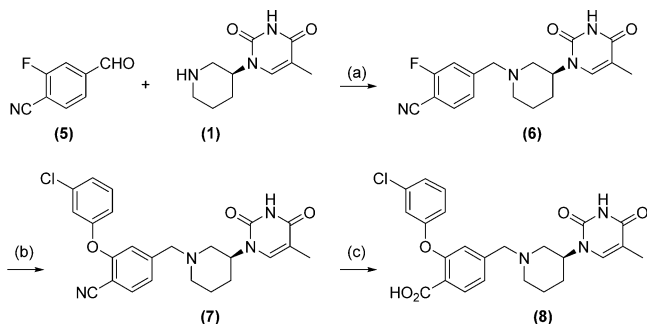
In our search for conserved residues across Gram-positive bacteria, Arg48 was identified as an attractive side chain to target. By the use of X-ray cocrystal structures and models, we predicted that placing an acid group at the C-4 of ring C would be optimal (Figure 4A). When synthesized and assayed, these acid derivatives showed more than a 20-fold improvement in IC$_{50}$ (Table 3). The X-ray cocrystal structure of compound **34** (Figure 4B) showed the formation of two clear hydrogen bonds between the carboxylate of **34** and the guanidinium of Arg48. As shown in Table 3, these compounds showed excellent IC$_{50}$ and MIC values against *S. pneumoniae*. The enzymatic IC$_{50}$ and MIC values for *S. aureus* were improved, but they remained more than 10-fold weaker than those of *S. pneumoniae*.

In order to improve the binding affinity against both *S. pneumoniae* and *S. aureus* TMK, the next area targeted was the methylene linker between ring B and ring C. Based on the X-ray structures and models, we hypothesized that adding a substituent to this carbon should have a positive effect by stabilizing the U-shaped binding conformation. The addition of a small group, such as a methyl (**35**), led to an improvement in the affinity for *S. aureus* TMK of more than 10-fold (Table 4). Although the enzyme affinities for both *S. pneumoniae* and *S. aureus* TMK were now comparable, the MICs for *S. aureus* were relatively weaker than those for *S. pneumoniae*. At this point, we established the link between enzyme inhibition and observed MICs through resistant mutant generation, radioactive-
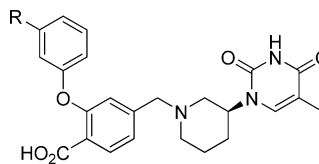
Table 2. TMK Inhibition Activity of Analogues of 4

Compound	R	*S. pneumoniae* IC$_{50}$ (nM)	*S. aureus* IC$_{50}$ (nM)
S-4	(phenyl)	2900	124000
S-20	(3-methylphenyl)	300	2700
S-21	(3-fluorophenyl)	400	3200
S-22	(3-chlorophenyl)	150	1200
S-23	(3-bromophenyl)	100	600
S-24	(2-chloro-methylphenyl)	1000	1900
S-25	(3-chloro-5-fluorophenyl)	100	2100
S-26	(3,5-dichlorophenyl)	400	1500
S-27	(4-chlorophenyl)	400	8500
R-28	(4-chlorophenyl)	5100	>200000
S-29	(3,4-dichlorophenyl)	400	2600
R-30	(2,3-dichlorophenyl)	18000	>200000

Scheme 2. Synthesis of TMK Inhibitors in Table 3[a]

[a](a) DMF, AcOH, polymer-BCN(H)$_3$, 22 °C, 16 h, 28%; (b) 3-chlorophenol, K$_2$CO$_3$, NMP, 150 °C, 15 min, 45%; (c) H$_2$SO$_4$, 150 °C, 30 min, 9%.

precursor incorporation assays, and *tmk* overexpression strains.[7] The compounds were found to exert their growth-inhibitory effect cleanly in both *S. aureus* and *S. pneumoniae* through TMK inhibition.

Table 3. Activity of Analogues of 34

| compd	R	IC$_{50}$ (nM)		log *D*	MIC (µg/mL)[a]	
		Spn	Sau		Spn	SauMSQS/SauMRQR
8	Cl	1.9	73	−0.55	1	32/32
31	Br	1	27	−0.51	1	16/32
32	Me	8	114	−0.82	4	64/128
33	F	28	339	−1	32	128/128
34	CF$_3$	10	120	−0.38	4	64/64

[a]Bacterial strains from the AstraZeneca collection. MSQS: methicillin- and quinolone-sensitive. MRQR: methicillin- and quinolone-resistant.

In an effort to improve whole-cell activity, we examined the physical properties of the series. *S. aureus* membrane permeability appears to be highly dependent on the physical properties of the molecules. In our experience, there is a good correlation between log *D* and the *S. aureus* MICs, with optimal whole-cell activity observed for log *D* values between 1 and 2.[10] Profiling of compounds **35−40** (Table 4) showed log *D* values between −0.3 and 0.5. In order to increase the log *D*, a series of compounds with substituents of increasing size and lipophilicity at the carbon linker between rings B and C were designed using calculated log *D* values and then synthesized (Scheme 3). As the size of the substituent increased, the (*R*) configuration of the new stereocenter became increasingly favored (Table 4, **39−43**). The X-ray structure of compound **41** showed that the binding mode was unchanged compared to our first X-ray cocrystal structure with all major interactions maintained (Figure 5). The source of affinity difference between the (*R,S*) and (*S,S*) diastereomers may be explained by the ability of the linker side chain in the (*R*) configuration to establish a hydrophobic interaction with Val51 and Leu52. Under the crystallization conditions, the enzyme also selectively bound the (*R,S*)-diastereomer when the diastereomeric mixture of **41/42** was used.

As shown in Table 4, the MICs against *S. aureus* improved as the log *D* increased from 0 to 2. For example, compound **47** exhibited excellent MICs against *S. aureus* (0.1−0.03 µg/mL) and a log *D* value of 2. On the other hand, compound **51** exhibited only a modest improvement in *S. aureus* MIC (0.5 µg/mL) in spite of the highest log *D* (2.5), indicating a limit to lipophilicity-induced gains in whole-cell activity for this series (Figure 6).

Compounds **14** (TK-666)[7] and **46** in Table 5 were profiled against pathogens *S. aureus*, *S. pneumoniae*, *Streptococcus pyogenes*, *Staphylococcus epidermidis*, and *Enterococcus* spp., showing excellent activity and demonstrating the value of a novel antibacterial target and mechanism for addressing serious exisiting clinical resistance mechanisms. Finally, for any novel antibacterial target with an essential eukaryotic ortholog, it is critical that selectivity be robust to avoid potential toxicity. Several compounds were thus tested in the human TMK IC$_{50}$ assay and showed exquisite (10^5−10^6) selectivity against the human homologue as well as very low potential for cytotoxicity in both human (A459) and yeast whole-cell assays (Table 6). Compound **14** was further dosed in a murine *S. aureus*-infected thigh model and demonstrated both efficacy (infection stasis at
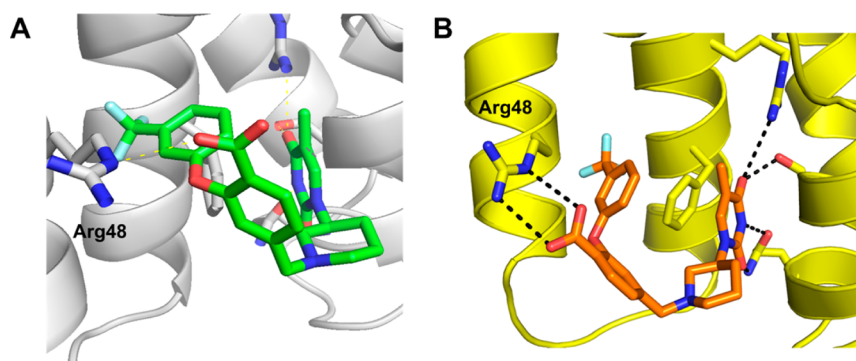
Figure 4. Structural characterization of the binding of **34** in *S. aureus* TMK. The addition of a carboxylate group to ring C was designed to specifically interact with the side chain of conserved Arg48. This carboxylate drove significant improvements in potency and physical properties. (A) Computational model of the carboxylate-Arg48 interaction predicted a single hydrogen bond. (B) Crystal structure, resolved to 1.7 Å. The carboxylic acid interaction with Arg48 is revealed to be bidentate.

Scheme 3. Synthesis of TMK Inhibitors in Table 4[a]
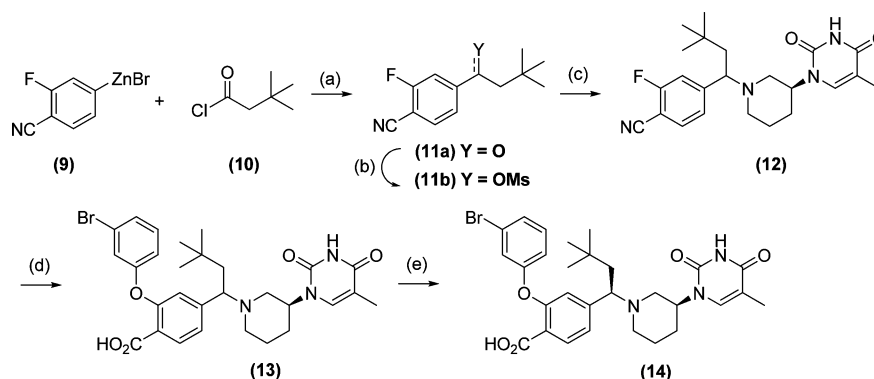
[a]Pd(PPh₃)₄, THF; 22 °C, 16 h, 85%; (b) (i) NaBH₄, MeOH, 22 °C, 2 h, 29%; (ii) MsCl, TEA, THF, 0 °C, 4 h; (c) (S)-**1**, **11b**, DIEA, CH₃CN, 70 °C, 20 h, 13%; (d) (i) 3-bromophenol, K₂CO₃, NMP, 150 °C, 30 min, 67%; (ii) NaOH, H₂O, EtOH, 100 °C, 16 h, 77%; (e) purification/separation by chiral chromatography, 15%.

150 mg/kg single dose, versus 40 mg/kg for comparator levofloxacin) and tolerability (no observed adverse effects up to and including the highest dose of 800 mg/kg/day).[7]

CONCLUSIONS

In this report we have illustrated the use of X-ray crystallography, computational methods, and traditional medicinal chemistry approaches to design the first potent, efficacious inhibitors of Gram-positive bacterial thymidylate kinase. After a small number of design cycles, the weak lead inhibitor **16** was rapidly optimized into the highly selective picomolar inhibitor **14**. While excellent cellular potency was easily obtained against *S. pneumoniae*, improving cellular activity against *S. aureus* proved to be more challenging due to the sensitivity of this species to the physical properties of the inhibitor. By utilizing the bridge carbon between rings B and C, log *D* adjustments were made which allowed us to improve some enzymatic potency but, more importantly, led to on-target, potent cellular activity against *S. aureus*. Compounds **14** and **46** showed excellent antibacterial spectrum against Gram-positive bacteria and 10^5−10^6 selectivity versus the human thymidylate kinase homologue. The *in vivo* target validation provided by compound **14**[7] against *S. aureus* provides great impetus for the development of clinical candidates both in the series and for the TMK target.
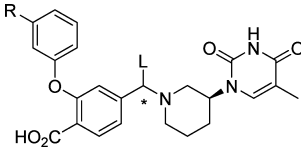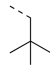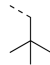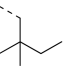
EXPERIMENTAL SECTION
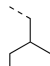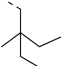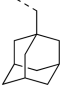
General Experimental Details. All commercial reagents and anhydrous solvents were obtained from commercial sources and were used without further purification, unless otherwise specified.

LC-MS conditions: *Method 1:* Samples were analyzed by reversed phase LC-MS using Waters Xterra C18 MS 100 mm × 4.6 mm, 5 μm particle size columns; linear gradient from 5% to 95% acetonitrile in water (10 mM ammonium hydrogen carbonate) over 5.5 min; flow rate 2 mL/min; injection volume was 2−7 μL; UV detection via HP or Waters DAD (210−400 nm range). Detection was based on ESCI in positive and negative polarity using a Micromass ZQ single quadrupole LC-MS or Quattro Micro LC-MS-MS, diode-array UV detector from 210 to 400 nm via HP or Waters DAD. *Method 2:* Samples were analyzed by reversed phase LC-MS using Varian Polaris C18A, 2 mm × 50 mm, 3 μm particle size columns. An Agilent HP1100 (Wimington, DE, USA) LC system was used with a gradient elusion profile of 5−95% B over 4.5 min at 1 mL/min, then re-equilibration at initial conditions to 6 min. Injection volume was 2 μL and column temperature 30 °C. Mobile phase A was 0.1% formic acid in water and mobile phase B 0.1% formic aci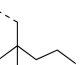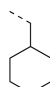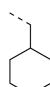d in acetonitrile. Detection was based on electrospray ionization (ESI) in positive and negative polarity using Waters ZQ mass spectrometer (Milford, MA, USA), diode-array UV detector from 210 to 400 nm, and evaporative light-scattering detector (Sedex 75, Sedere, Alfortville Cedex, France). *Method 3:* As Method 2, except A was 10 mM ammonium acetate in (5/95 acetonitrile/water) and B was acetonitrile.

Accurate mass was done using a hybrid quadrupole time-of-flight mass spectrometer (microTOFQ, Bruker Daltonics) in ESI+ mode. Method: 5−95% mobile phase B from 0.0 to 5.0 min, hold at 95%

Table 4. Activity of Single Diastereomer Analogues of 41


| Compound | R | L | IC$_{50}$ (nM) | | | MIC (μg/mL)[a] | |
			Spn	Sau	log D	Spn	SauMSQS/SauMRQR
(*R*,*S*)-35	Cl	Me	0.3	2.5	-0.26	0.1	4/8
(*S*,*S*)-36	Cl	Me	1	29.3	-0.3	0.25	8/8
(*R*,*S*)-37	Cl	Et	0.6	13.7	0.2	0.1	2/2
(*S*,*S*)-38	Cl	Et	3	18.3	0.2	0.25	2/4
(*R*,*S*)-39	Cl	Pr	0.3	8.3	0.6	0.05	1/1
(*S*,*S*)-40	Cl	Pr	0.6	18	0.5	0.1	4/4
(*R*,*S*)-41	Cl	*i*-Bu	<0.2	1.2	0.9	0.03	1/1
(*S*,*S*)-42	Cl	*i*-Bu	0.6	13.5	0.9	0.05	2/2
(*R*,*S*)-14	Br		0.2	0.8	1.1	0.02	0.25/0.25
(*S*,*S*)-43	Br		0.6	2.8	1.2	0.03	2/1
(*R*,*S*)-44	Cl		0.3	1.0	1.4	0.05	0.25/0.1
(*R*,*S*)-45	Cl		0.1	<3	1.7	0.02	0.25/0.1
(*R*,*S*)-46	Br	Pentyl	<0.1	0.5	1.1	0.01	0.25/0.1
(*R*,*S*)-47	Br		0.3	1.3	2	0.03	0.1/0.03
(*R*,*S*)-48	Cl		0.3	0.7	2	0.06	0.25/0.06
(*R*,*S*)-49	Cl		<0.1	0.7	1.8	0.01	0.25/0.1
(*R*,*S*)-50	Cl		<0.1	1.6	-0.25	0.1	16/8
(*R*,*S*)-51	Br		0.1	1.1	2.5	0.03	0.25/0.1

[a]Bacterial strains from the AstraZeneca collection. MSQS: methicillin- and quinolone-sensitive. MRQR: methicillin- and quinolone-resistant.

mobile phase B to 5.1 min. Mobile phase A: 0.1% formic acid in water, B: 0.1% formic acid in acetonitrile. 1.0 mL/min flow, column Varian Polaris C18-A 2.0 mm × 50 mm, 3.0 μm particle size. One μL of sample was injected onto an HPLC using an externally calibrated instrument for accurate mass measurement. 50 μL/min eluent from LC and 50 μL/min make up solution (CH$_3$CN/H$_2$O 50/50) went into MS.

^{1}H NMR spectra (δ, ppm) were recorded using Bruker Advance Ultrashield 300 MHz or Bruker DPX 400 MHz instruments.

Column chromatography was performed using Silcycle FLH-R10030B Silisep cartridges (12−330 g). Preparative reversed phase HPLC chromatography was carried out using a Waters Atlantis T3-C18 column, 19 mm × 100 mm, 5 μm, a linear gradient from 10% to 90% CH$_3$CN in H$_2$O over 12 min (0.1% trifluoroacetic acid), and a
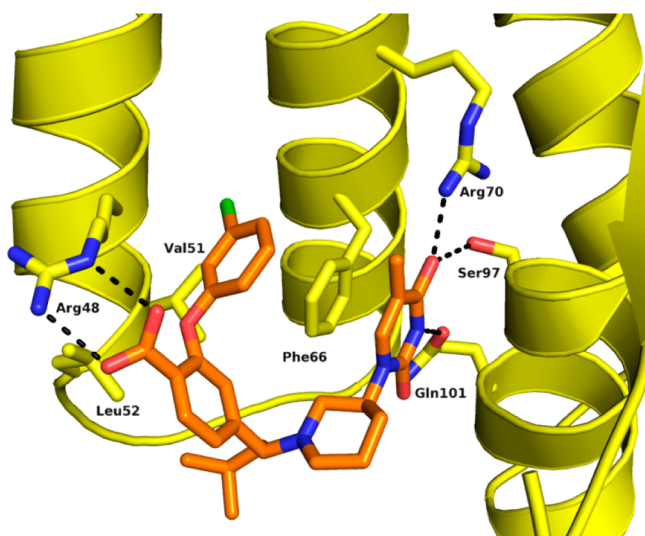
Figure 5. Co-crystal structure of a single diastereomer (R,S)-**41** and S. aureus TMK at 2.0 Å, depicting optimized inhibitor binding to the enzyme (IC$_{50}$ = 1.2 nM). Key features are retention of thymine binding interactions (ring A), hydrophobic packing of the isobutyl group against conserved hydrophobic residues Val51/Leu52 (linker between rings B and C), the bidentate salt bridge of the ring C carboxylate to Arg48, and the cryptic hydrophobic pocket hosting the chlorophenyl ring D. The π-stack of rings A and D with Phe66 is maintained.
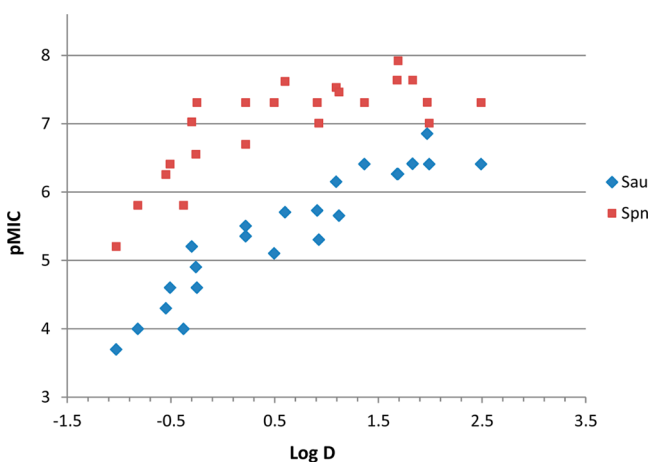
Figure 6. pMIC vs log D relationship for piperidinylthymine analogs in Table 4. S. aureus appears to be more sensitive to log D variation than S. pneumoniae, but both reach an MIC optimum with log D between 1.5 and 1.8.

flow rate of 20 mL/min. Preparative chiral chromatography was carried out as follows. *HPLC:* Chiralpak IC column, 30 mm × 250 mm, 5 μm; hexane (60%), methanol/ethanol (1:1) (40%), 0.5% diethylamine; flow rate 40 mL/min. *SFC:* Chiralpak AD column, 30 mm × 250 mm, 5 μm; carbon dioxide (60%), isopropanol (40%); flow rate 120 mL/min. Chiral analytical HPLC: Chiralpak IC column, 4.6 mm × 250 mm, 5 μm; hexane (60%), methanol/ethanol (1:1) (40%), 0.5% diethylamine; flow rate 1 mL/min. Chiral analytical SFC: Chiralpak AD column, 4.6 mm × 250 mm, 5 μm; carbon dioxide (60%), isopropanol (40%); flow rate 2.8 mL/min.

The purity of the final compounds was assessed on the basis of analytical LC-MS, and the results were greater than 95% unless specified otherwise.

Molecular Modeling. Molecular docking was performed using Glide version 5.0[13] in standard flexible docking mode. X-ray structures

Table 5. Gram-Positive Antibacterial Spectrum of Analogues 14 and 46

	MIC (μg/mL)	
bacterial strain[a]	(R,S)-14	(R,S)-46
S. pneumoniae	0.02	0.01
Streptococcus pyogenes	0.08	0.04
S. aureus MSQS/S. aureus MRQR	0.25/0.25	0.25/0.1
Staphylococcus epidermidis	2	0.5
Enterococcus faecium (LRE)	0.25	0.25
Enterococcus faecalis (VRE)	1	0.06

[a]Bacterial strains from AstraZeneca collection. MSQS: methicillin- and quinolone-sensitive; MRQR: methicillin- and quinolone-resistant; LRE: linezolid-resistant *Enterococcus*; VRE: vancomycin-resistant *Enterococcus*.

Table 6. Eukaryotic Selectivity for Selected Analogues

	IC$_{50}$ (nM)	MIC (μg/mL)	
	Human TMK	Human A549[a]	Candida albicans
34	>200000	>64	>64
(R,S)-**35**	150000	>64	>64
(R,S)-**39**	150000	>64	>64
(R,S)-**14**	62000	>64	>64
(R,S)-**44**	43400	>64	>64
(R,S)-**46**	32000	>64	>64

[a]Human A549: Human lung epithelial adenocarcinoma cell line.

of Sau-TMK protein in complex with related ligands were used as a template for docking studies. The protein structures were prepared using protein preparation wizard, and the ligands were prepared using Ligprep utility in Maestro 8.5 (Schrodinger, LLC 2008, New York, NY). Docked poses were minimized in OPLS 2001[14] force field as implemented in Maestro 8.5.

Experimental Procedures and Characterization Data for Analogues in Tables 1 and 2. *5-Methyl-1-(piperidin-3-yl)-pyrimidine-2,4(1H,3H)-dione (1).*[15c] Oxalyl chloride (24 mL) was added to a mixture of (E)-3-methoxy-2-methylacrylic acid[15] (**2**, 42 g, 0.25 mol, 1.0 equiv) in dichloromethane (250 mL) at 0 °C. The mixture was stirred at room temperature for 1 h. The solvent was removed under reduced pressure. The resultant residue was redissolved in toluene (750 mL), and silver cyanate (48.75 g, 0.325 mol, 1.3 equiv) was added. The reaction mixture was stirred at 95 °C for 3 h and allowed to cool to RT, and the inorganics were filtered. Filtrate was added slowly to a solution of (S)-tert-butyl 3-amino-piperidine-1-carboxylate (**3**, 50 g, 0.25 mol, 1.0 equiv) in dimethyl formamide (100 mL). The mixture was stirred at room temperature for 16 h. The solvent was removed under reduced pressure. The residue was dissolved in diethyl ether (750 mL) and washed with water (2 × 250 mL), 10% aqueous NaHCO$_3$ (1 × 250 mL), and brine (1 × 100 mL), dried over Na$_2$SO$_4$, and filtered, and the solvent was removed under reduced pressure to afford (S)-tert-butyl (3-3-(((2E)-3-methoxy-2-methylprop-2-enoyl)carbamoyl)amino)piperidine-1-carboxylate, as a pale yellow solid (53 g). ^{1}H NMR (400 MHz, DMSO-d$_6$) δ 1.40 (s, 9H), 1.40−165 (m, 3H), 1.65 (s, 3H), 1.83 (m, 1H), 3.24 (m, 2H), 3.43 (m, 2H), 3.70 (m, 1H), 3.83 (s, 3H), 7.50 (s, 1H), 8.81 (d, 1H), 9.78 (s, 1H) ppm. A 1.69 N aqueous solution of sulfuric acid (800 mL) was added to a mixture of (S)-(E)-tert-butyl 3-(3-(3-methoxy-2-methylacryloyl)ureido)piperidine-1-carboxylate (53 g, 0.155 mol) and 1,4-dioxane (300 mL). The mixture was stirred at 95 °C for 16 h. The reaction mixture was allowed to cool to room temperature and slowly neutralized with addition of solid sodium hydrogen carbonate (200 g). The reaction mixture was concentrated to dryness, and the residue was extracted with hot methanol. The methanol was concentrated, and the residue was purified by column chromatography to afford **1** as a pale yellow solid (20.7 g, 40% overall yield from 2 steps). ^{1}H NMR (400 MHz, CD$_3$OD) δ 1.84−1.96 (m,

6H), 2.54 (dt, *J* = 2.60, 12.66 Hz, 1H), 2.74 (t, *J* = 11.60 Hz, 1H), 2.80−3.10 (m, 3H), 4.43−4.48 (m, 1H), 7.53 (s, 1H). ¹H NMR (400 MHz, DMSO-*d*₆): δ 1.60−1.68 (m, 1H), 1.76 (s, 3H), 1.78−1.85 (m, 3H), 2.54−2.60 (m, 1H), 2.85−2.94 (m, 3H), 2.98−3.06 (m,1H), 4.46−4.54 (m, 1H), 7.66 (s, 1H), 11.20 (br s, 1H) ppm.

5-Methyl-1-(1-(3-phenoxybenzyl)piperidin-3-yl)pyrimidine-2,4-(1H,3H)-dione (4). A mixture of 5-methyl-1-(piperidin-3-yl)-pyrimidine-2,4(1H,3H)-dione (**1**, 100 mg, 0.48 mmol), 3-(phenoxy)-benzaldehyde (285 mg, 1.44 mmol), and (polystyrylmethyl)-trimethylammonium cyanoborohydride (200 mg, 0.8 mmol) in dichloromethane/acetic acid (90:10 v/v, 4 mL) was stirred at room temperature for 16 h. The reaction mixture was concentrated under reduced pressure, and the crude product was purified by reverse phase preparative HPLC to afford the title compound as a white solid (18 mg, 19%). LC-MS (Method 1) *t*ᵣ = 3.43 min, *m/z* = 392 (M + 1). HRMS calcd for C₂₃H₂₆N₃O₃ 392.1969, found 392.1969. ¹H NMR (400 MHz, DMSO-*d*₆) δ 1.55 (m, 1H), 1.68−1.80 (s, 6H), 2.05 (t, 1H), 2.20 (t, 1H), 2.70 (m, 2H), 3.55 (s, 2H), 4.45 (m, 1H), 6.95 (d, 1H), 7.00−7.20 (m, 5H), 7.35−7.42 (m, 3H), 7.74 (m, 1H), 11.23 (s, 1H) ppm.

5-Methyl-1-(1-(3-phenoxybenzyl)piperidin-3-yl)pyrimidine-2,4-(1H,3H)-dione (15). LC-MS (Method 1) *t*ᵣ = 3.43 min, *m/z* = 392 (M + 1). HRMS calcd for C₂₃H₂₆N₃O₃ 392.1969, found 392.1969. ¹H NMR (400 MHz, DMSO-*d*₆) δ 1.55 (m, 1H), 1.68−1.80 (s, 6H), 2.05 (t, 1H), 2.20 (t, 1H), 2.70 (m, 2H), 3.55 (s, 2H), 4.45 (m, 1H), 6.95 (d, 1H), 7.00−7.20 (m, 5H), 7.35−7.42 (m, 3H), 7.74 (s, 1H), 11.23 (s, 1H) ppm.

5-Methyl-1-(1-(3-(3-(trifluoromethyl)phenoxy)benzyl)piperidin-3-yl)pyrimidine-2,4(1H,3H)-dione (16). LC-MS (Method 1) *t*ᵣ = 3.86 min, *m/z* = 460 (M + 1), 458 (M − 1). HRMS calcd for C₂₄H₂₅F₃N₃O₃ 460.1843, found 460.1842. ¹H NMR (400 MHz, DMSO-*d*₆) δ 1.57 (m, 1H), 1.66−1.83 (m, 3H), 1.83 (s, 3H), 2.08 (t, 1H), 2.24 (t, 1H), 2.69−2.83 (m, 2H), 3.57 (s, 2H), 4.38−4.46 (m, 1H), 7.02 (dd, 1H), 7.08 (s, 1H), 7.19 (d, 1H), 7.32 (d, 2H), 7.43 (t, 1H), 7.51 (d, 1H), 7.65 (t, 1H), 7.74 (s, 1H), 11.22 (s, 1H) ppm.

5-Methyl-1-{1-[3-(4-methylphenoxy)benzyl]piperidin-3-yl}-pyrimidine-2,4(1H,3H)-dione (17). LC-MS (Method 2) *t*ᵣ = 2.64 min, *m/z* = 406.4 (M + 1). HRMS calcd for C₂₄H₂₈N₃O₃ 406.2125, found 406.2130. ¹H NMR (400 MHz, CDCl₃): δ 1.68−1.74 (m, 3H), 1.80−1.82 (m, 1H), 1.90 (s, 3H), 2.34 (m, 5H), 2.58 (m, 1H), 2.77−2.79 (m, 1H), 3.49 (q, *J* = 13.20 Hz, 2H), 4.58−4.60 (m, 1H), 6.86−7.02 (m, 5H), 7.14 (d, *J* = 8.40 Hz, 2H), 7.23−7.28 (m, 1H), 7.69 (s, 1H), 8.12 (s, 1H) ppm.

1-(1-(3-(4-Chlorophenoxy)benzyl)piperidin-3-yl)-5-methylpyrimidine-2,4(1H,3H)-dione (18). LC-MS (Method 2) *t*ᵣ = 2.71 min, *m/z* = 426, 428 (M + 1, M + 2). HRMS calcd for C₂₃H₂₅ClN₃O₃ 426.1583, found 426.1577. ¹H NMR (400 MHz, CDCl₃): δ 1.69−1.86 (m, 4H), 1.91 (s, 3H), 2.35 (m, 2H), 2.62 (m, 1H), 2.79−2.81 (m, 1H), 3.51 (q, *J* =13.20 Hz, 2H), 4.58−4.60 (m, 1H), 6.89−6.90 (m, 3H), 7.01 (s, 1H), 7.06−7.08 (m, 1H), 7.28−7.32 (m, 3H), 7.62 (m, 1H), 8.13 (s, 1H) ppm.

1-(1-(3-(4-Methoxyphenoxy)benzyl)piperidin-3-yl)-5-methylpyrimidine-2,4(1H,3H)-dione (19). LC-MS (Method 2) *t*ᵣ = 2.50 min, *m/z* = 422.1 (M + 1). HRMS calcd for C₂₄H₂₈N₃O₄ 422.2074, found 422.2072. ¹H NMR (400 MHz, CDCl₃): δ 1.66−1.75 (m, 3H), 1.81−1.83 (m, 1H), 1.91 (s, 3H), 2.37−2.42 (m, 2H), 2.59 (m, 1H), 2.78 (dd, *J* =3.68, 11.34 Hz, 1H), 3.49 (q, *J* =13.20 Hz, 2H), 3.82 (s, 3H), 4.57−4.60 (m, 1H), 6.82 (dd, *J* = 1.84, 8.12 Hz, 1H), 6.88−6.93 (m, 3H), 6.96−7.00 (m, 3H), 7.22−7.25 (m, 1H), 7.67 (s, 1H), 8.05 (s, 1H) ppm.

(S)-5-Methyl-1-(1-(3-(m-tolyloxy)benzyl)piperidin-3-yl)-pyrimidine-2,4(1H,3H)-dione (20). LC-MS (Method 2) *t*ᵣ = 2.70 min, *m/z* = 406.2 (M). HRMS calcd for C₂₄H₂₈N₃O₃ 484.1634, found 406.2105. ¹H NMR (300 MHz, DMSO-*d*₆) δ 1.60 (m, 1H), 1.65−1.80 (s and m, 6H), 2.05 (t, 1H), 2.20 (t, 1H), 2.54 (m, 2H), 3.50 (s, 2H), 4.40 (m, 1H), 6.95 (m, 1H), 7.01 (m's, 2H), 7.15 (m's, 2H), 7.33 (m, 2H), 7.37 (t, 1H), 7.71 (s, 1H), 11.2 (br s, 1H) ppm.

(S)-1-(1-(3-(3-Fluorophenoxy)benzyl)piperidin-3-yl)-5-methylpyrimidine-2,4(1H,3H)-dione (21). LC-MS (Method 2) *t*ᵣ = 2.77 min, *m/z* = 410.1 (M + 1). ¹H NMR (400 MHz, CD₃OD) δ 1.60−1.88 (s and m, 7H), 2.23 (t, 1H), 2.35 (t, 1H), 2.75 (m, 1H), 2.83 (m, 1H), 3.57

(s, 2H), 4.57 (m, 1H), 6.78 (m, 1H), 6.83 (m, 1H), 6.96 (m, 1H), 7.06 (m, 1H), 7.16 (d, 1H), 7.34 (m, 2H), 7.74 (s, 1H) ppm.

(S)-1-(1-(3-(3-Chlorophenoxy)benzyl)piperidin-3-yl)-5-methylpyrimidine-2,4(1H,3H)-dione (22). LC-MS (Method 2) *t*ᵣ = 1.90 min, *m/z* = 426.1 (M + 1). ¹H NMR (300 MHz, CD₃OD) δ 1.47−1.87 (m, 7H) 2.00−2.34 (m, 2H), 2.63 (br s, 1H), 2.68−2.84 (m, 1H), 3.47 (s, 2H), 4.45 (br s, 1H), 6.70−6.88 (m, 3H), 6.88−7.13 (m, 3H), 7.13−7.32 (m, 2H), 7.64 (br s, 1H) ppm.

(S)-1-(1-(3-(3-Bromophenoxy)benzyl)piperidin-3-yl)-5-methylpyrimidine-2,4(1H,3H)-dione (23). LC-MS (Method 2) *t*ᵣ = 3.04 min, *m/z* = 469.8 471.7 (M + 1, M + 3). HRMS calcd for C₂₃H₂₅BrN₃O₃ 470.1074, found 470.1057. ¹H NMR (400 MHz, DMSO-*d*₆) δ 1.60 (m, 1H), 1.65−1.80 (s and m, 6H), 2.05 (t, 1H), 2.20 (t, 1H), 2.54 (m, 2H), 3.50 (s, 2H), 4.40 (m, 1H), 6.95 (m, 1H), 7.01 (m's 2H), 7.15 (m's, 2H), 7.33 (m, 2H), 7.37 (t, 1H), 7.71 (s, 1H), 11.2 (br s, 1H) ppm.

(S)-1-(1-(3-(3-Chloro-4-methylphenoxy)benzyl)piperidin-3-yl)-5-methylpyrimidine-2,4(1H,3H)-dione (24). LC-MS (Method 2) *t*ᵣ = 3.19 min, *m/z* = 439.95, 441.88 (M + 1, M + 3). HRMS calcd for C₂₄H₂₇ClN₃O₃ 440.1735, found 440.1723. ¹H NMR (400 MHz, CD₃OD) δ 1.66−1.90 (s and m, 7H), 2.23 (m, 1H), 2.33 (m, 4H), 2.73 (m, 1H), 2.85 (m, 1H), 3.55 (s, 2H), 4.55 (m, 1H), 6.83 (m, 1H), 6.83 (m, 1H), 6.91 (m, 1H), 6.94 (d, 1H), 7.00 (m, 1H), 7.11 (d, *J* = 7.83, 1H), 7.24 (d, *J* = 8.34, 1H), 7.33 (d, *J* = 7.83, 1H) 7.75 (s, 1H) ppm.

(S)-1-(1-(3-(3-Chloro-5-fluorophenoxy)benzyl)piperidin-3-yl)-5-methylpyrimidine-2,4(1H,3H)-dione (25). LC-MS (Method 1) *t*ᵣ = 1.86 min, *m/z* = 444.1 (M + 1), 442.3 (M − 1). HRMS calcd for C₂₃H₂₄ClFN₃O₃ 444.1485, found 444.1487. ¹H NMR (300 MHz, CD₃OD) δ 1.48−1.81 (m, 7H), 2.13 (br s, 1H), 2.24 (t, *J* = 10.17 Hz, 1H), 2.65 (d, *J* = 11.30 Hz, 1H), 2.76 (dd, *J* = 10.55, 3.77 Hz, 1H), 3.49 (s, 2H), 4.36−4.55 (m, 1H), 6.56 (d, *J* = 10.55 Hz, 1 H), 6.66 (s, 1H), 6.81 (d, *J* = 8.29 Hz, 1H), 6.90 (d, *J* = 8.29 Hz, 1H), 6.99 (s, 1H), 7.11 (d, *J* = 7.54 Hz, 1H), 7.30 (t, *J* = 7.91 Hz, 1H), 7.65 (s, 1H) ppm.

(S)-1-(1-(3-(3,5-Dichlorophenoxy)benzyl)piperidin-3-yl)-5-methylpyrimidine-2,4(1H,3H)-dione (26). LC-MS (Method 2) *t*ᵣ = 1.92 min, *m/z* = 460.1, 462.5 (M, M + 2). HRMS calcd for C₂₃H₂₄Cl₂N₃O₃ 460.1189, found 460.1184. ¹H NMR (300 MHz, CD₃OD) δ 1.83 (m, 7H), 2.28 (dt, 2H), 2.8 (dm, 2H), 3.58 (s, 2H), 4.55 (m, 1H), 6.89 (m, 2H), 6.93 (d, 1H), 7.08 (s, 1H), 7.15 (s, 1H), 7.28 (m, 1H), 7.39 (m, 1H), 7.74 (s, 1H) ppm.

(S)-1-(1-(3-(4-Chlorophenoxy)benzyl)piperidin-3-yl)-5-methylpyrimidine-2,4(1H,3H)-dione (27). LC-MS (Method 2) *t*ᵣ = 1.96 min, *m/z* = 426.1 (M + 1). HRMS calcd for C₂₃H₂₅ClN₃O₃ 426.1579, found 426.1570. ¹H NMR (300 MHz, DMSO-*d*₆) δ 1.79 (m, 7H), 2.82 (s, 1H), 3.17 (m, 1H), 3.42 (t, 2H), 4.32 (m, 2H), 4.72 (br t, 1H), 7.08 (s, 1H), 7.10 (s, 1H), 7.20 (d, 1H), 7.24 (s, 1H), 7.37 (d, 1H), 7.43−7.55 (m, 4H), 9.9 (br s, 1H), 11.4 (s, 1H) ppm.

(R)-1-(1-(3-(4-Chlorophenoxy)benzyl)piperidin-3-yl)-5-methylpyrimidine-2,4(1H,3H)-dione (28). LC-MS (Method 2) *t*ᵣ = 1.82 min, *m/z* = 428.3 (M + 1). HRMS calcd for C₂₃H₂₅ClN₃O₃ 426.1579, found 426.1583. ¹H NMR (300 MHz, CD₃OD) δ 1.54−1.93 (m, 7H), 2.05−2.42 (m, 2H), 2.63−2.96 (m, 2H), 3.55 (br s, 2H), 4.55 (d, *J* = 3.77 Hz, 1H), 6.78−7.05 (m, 4H), 7.10 (d, *J* = 7.54 Hz, 1H), 7.33 (d, *J* = 4.52 Hz, 3H), 7.72 (br s, 1H) ppm.

(S)-1-(1-(3-(3,4-Dichlorophenoxy)benzyl)piperidin-3-yl)-5-methylpyrimidine-2,4(1H,3H)-dione (29). LC-MS (Method 2) *t*ᵣ = 2.29 min, *m/z* = 460.0, 461.9 (M + 1 M + 3). HRMS calcd for C₂₃H₂₄Cl₂N₃O₃ 460.1189, found 460.1190. ¹H NMR (300 MHz, DMSO-*d*₆) δ 1.75 (s, 3H), 1.90 (m, 4H), 2.85 (m, 1H), 3.20 (m, 1H), 3.45 (t, 2H), 4.30 (m, 2H), 4.75 (t, 1H), 7.07 (m, 1H), 7.20 (d, 1H), 7.35 (m's, 3H), 7.55 (m's, 2H), 7.85 (d, 1H), 10.6 (br s, 1H), 11.35 (s, 1H) ppm.

(R)-1-(1-(3-(3,4-Dichlorophenoxy)benzyl)piperidin-3-yl)-5-methylpyrimidine-2,4(1H,3H)-dione (30). LC-MS (Method 2) *t*ᵣ = 2.04 min, *m/z* = 461.9 (M + 1), 458.3 (M − 1). HRMS calcd for C₂₃H₂₄Cl₂N₃O₃ 460.1189, found 460.1187. ¹H NMR (300 MHz, CD₃OD) δ 1.54−1.94 (m, 7H), 2.10−2.40 (m, 2H), 2.75 (d, *J* = 11.30 Hz, 1H), 2.80−2.92 (m, 1H), 3.20−3.45 (m, 2H), 3.45−3.67 (m, 2H), 4.54 (br s, 1H), 6.76−7.00 (m, 2H), 7.00−7.26 (m, 3H), 7.26−7.58 (m, 2H), 7.72 (br s, 1H) ppm.

Experimental Procedures and Characterization Data for Analogues in Table 3. *(S)-2-Fluoro-4-((3-(5-methyl-2,4-dioxo-3,4-dihydropyrimidin-1(2H)-yl)piperidin-1-yl)methyl)benzonitrile (6).* (S)-5-Methyl-1-(piperidin-3-yl)pyrimidine-2,4(1H,3H)-dione (**1**, 1052 mg, 5.03 mmol), cyanoborohydride on resin (2515 mg, 5.03 mmol), and 2-fluoro-4-formylbenzonitrile (**5**, 500 mg, 3.35 mmol) were suspended in DMF (10 mL). Acetic acid (0.500 mL) was added, and the mixture was stirred at RT overnight. LCMS showed product. The resin was removed by filtration, and the crude was then diluted in ethyl acetate, washed with saturated aqueous sodium bicarbonate and water, and then dried over anhydrous sodium sulfate. After the solvent was removed under reduced pressure, the crude oil was purified by reverse phase chromatography HPLC (acetonitrile, water, 0.1% TFA) (5−50% acetonitrile). After the solvent was removed, a solid was isolated and identified as **6** (323 mg, 28%). LC-MS (Method 1) t_R = 0.88 min, m/z = 342.0, 344.0 (M, M + 2). ¹H NMR (300 MHz, CD₃OD) δ 1.82 (overlap m and s, 7H), 2.19 (m, 1H), 2.33 (t, J = 10.5 Hz, 1H), 2.78 (d, J = 10.5 Hz, 1H), 2.89 (dd, J = 10.5, 4.5 Hz, 1H), 3.67 (s, 2H), 4.59 (m, 1H), 7.39 (m, 2H), 7.71 (m, 2H) ppm.

(S)-2-(3-Chlorophenoxy)-4-((3-(5-methyl-2,4-dihydro-pyrimidin-1(2H)-yl)piperidin-1-yl)methyl)benzonitrile (7). 3-Chlorophenol (28.2 mg, 0.22 mmol), **6** (50 mg, 0.15 mmol), and anhydrous potassium carbonate (20.18 mg, 0.15 mmol) were suspended in N-methyl-2-pyrrolidinone (1 mL). The mixture was heated using a microwave oven at 150 °C for 15 min. The reaction mixture was then purified by preparative HPLC, eluting with mixtures of acetonitrile/water/0.1% TFA. The fractions containing clean product were mixed, and the solvent was removed under reduced pressure, yielding **7** (30.0 mg, 45%) as a solid. LC-MS (Method 1) t_R = 1.79 min, m/z = 451.1 (M + 1), 449.2 (M − 1).

(S)-2-(3-Chlorophenoxy)-4-((3-(5-methyl-2,4-dihydro-pyrimidin-1(2H)-yl)piperidin-1-yl)methyl)benzoic Acid (8). **7** (30 mg, 0.07 mmol) was suspended in water (1 mL). Sulfuric acid (0.100 mL) was added, and the sample was heated using microwave irradiation for 30 min at 150 °C. The crude was then purified using preparative HPLC, eluting with mixtures of acetonitrile/water/TFA 0.1%. The recovered clean fractions were combined, and the solvent was removed using the lyophilizer, yielding **8** (3.40 mg, 9%) as an off white solid. LC-MS (Method 1) t_R = 1.42 min, m/z = 470.1, 468.2 (M + 1, M − 1). HRMS calcd for $C_{24}H_{25}ClN_3O_5$ 470.1477, found 470.1469. ¹H NMR (300 MHz, CD₃OD) δ 1.89 (m, 4H), 2.08 (m, 3H), 3.0 (br t, 1H), 3.23 (apparent t, overlap with solvent signal, 1H), 3.5 (m, 2H), 4.38 (m, 2H), 4.67 (m, 1H), 6.9 (dd, J = 8.3, 1.1 Hz, 1H), 7.0 (t, J = 2.2 Hz, 1H), 7.13 (m, 1H), 7.24 (d, J = 1.5 Hz, 1H), 7.33 (m, 1H), 7.43 (m, 1H), 8.04 (d, J = 7.9 Hz, 1H) ppm.

(S)-2-(3-Bromophenoxy)-4-((3-(5-methyl-2,4-dioxo-3,4-dihydro-pyrimidin-1(2H)-yl)piperidin-1-yl)methyl)benzoic Acid (31). LC-MS (Method 2) t_R = 1.45 min, m/z = 514.0, 516.0 (M + 1, M + 3), 512.3 (M − 1). HRMS calcd for $C_{24}H_{25}BrN_3O_5$ 514.0972, found 514.0947. ¹H NMR (300 MHz, CD₃OD) δ 1.78−2.05 (m, 6H), 2.84 (t, 1H), 3.06 (t, 1H), 3.33 (m, 2H), 4.21 (m, 2H), 4.57 (br s, 1H), 6.85 (m, 1H), 7.03 (s, 1H), 7.15 (m, 1H), 7.34 (d, 1H), 7.39 (m, 1H), 7.92 (d, 1H) ppm.

(S)-4-((3-(5-Methyl-2,4-dioxo-3,4-dihydropyrimidin-1(2H)-yl)-piperidin-1-yl)methyl)-2-(m-tolyloxy)benzoic Acid (32). LC-MS (Method 2) t_R = 1.38 min, m/z = 450.3 (M + 1), 448.34 (M − 1). HRMS calcd for $C_{25}H_{28}N_3O_5$ 450.2023, found 450.2004. ¹H NMR (300 MHz, CD₃OD) δ 1.78 (s, 3H), 1.82−2.14 (m, 3H), 2.21 (s, 2H), 2.87 (br s, 1H), 3.10 (t, J = 11.68 Hz, 1H), 3.29−3.46 (m, 2H), 4.11−4.34 (m, 2H), 4.55 (dd, J = 10.55, 5.27 Hz, 1H), 6.68 (d, J = 7.54 Hz, 1H), 6.76 (s, 1H), 6.87 (d, J = 7.54 Hz, 1H), 7.02 (s, 1H), 7.13 (t, J = 7.54 Hz, 1H), 7.23 (d, J = 9.80 Hz, 1H), 7.32 (s, 1H), 7.88 (d, J = 8.29 Hz, 1H) ppm.

(S)-2-(3-Fluorophenoxy)-4-((3-(5-methyl-2,4-dioxo-3,4-dihydropyrimidin-1(2H)-yl)piperidin-1-yl)methyl)benzoic Acid (33). LC-MS (Method 2) t_R = 1.3 min, m/z = 454.3 (M + 1), 452.2 (M − 1). HRMS calcd for $C_{24}H_{25}FN_3O_5$ 454.1773, found 454.1759. ¹H NMR (300 MHz, CD₃OD) δ 1.47−1.81 (m, 7 H), 2.15 (br s, 1H), 2.28 (t, J = 10.17 Hz, 1H), 2.68 (d, J = 10.55 Hz, 1H), 2.79 (dd, J = 10.55, 3.77 Hz, 1H), 3.54 (s, 2H), 4.44 (br s, 1H), 6.49−6.76 (m, 3H), 6.97 (s, 1H), 7.17 (dd, J = 14.69, 7.16 Hz, 2H), 7.58 (s, 1H), 7.74 (d, J = 8.29 Hz, 1H) ppm.

4-((3-(5-Methyl-2,4-dioxo-3,4-dihydropyrimidin-1(2H)-yl)-piperidin-1-yl)methyl)-2-(3-(trifluoromethyl)phenoxy)benzoic Acid (34). LC-MS (Method 2) t_R = 2.46 min, m/z = 504.2 (M + 1). HRMS calcd for $C_{25}H_{25}FN_3O_5$ 504.1741, found 504.1742. ¹H NMR (400 MHz, DMSO-d_6): δ 1.48−1.53 (m, 1H), 1.65−1.71 (m, 3H), 1.73 (s, 3H), 2.03 (t, J = 10.04 Hz, 1H), 2.20 (t, J = 10.16 Hz, 1H), 2.66−2.76 (m, 2H), 3.57 (s, 2H), 4.35−4.39 (m, 1H), 7.09−7.14 (m, 3H), 7.29 (d, J = 8.08 Hz, 1H), 7.40 (d, J = 7.72 Hz, 1H), 7.56 (t, J = 7.88 Hz, 1H), 7.68 (s, 1H), 7.85 (d, J = 7.92 Hz, 1H), 11.19 (s, 1H), 12.88 (br s, 1H) ppm.

Experimental Procedures and Characterization Data for Analogs in Table 4. *1-(4-Cyano-3-fluorophenyl)-(3,3-dimethylbutyl)methanesulfonate (11b).* (4-Cyano-3-fluorophenyl)-zinc(II) bromide (**9**, 163 mL, 81.72 mmol) was added dropwise (over 20 min) to a suspension of 3,3-dimethylbutanoyl chloride (**10**, 10.37 mL, 74.29 mmol) and tetrakis(triphenylphosphine)palladium(0) (2.146 g, 1.86 mmol) in tetrahydrofuran (200 mL) at room temperature and under an atmosphere of nitrogen. The solution turned from pale orange to dark red overnight. The crude was diluted in ethyl acetate (200 mL) and washed with aqueous saturated sodium bicarbonate, water, and aqueous 1 N HCl. The organic extract was dried over anhydrous sodium sulfate, and the solvent was removed under reduced pressure, yielding a thick reddish oil containing a shiny solid. The crude oil was suspended in diethyl ether, and the solids were removed by filtration. The crude was then purified by flash chromatography on silica gel (330 g) eluting with mixtures of hexanes/ethyl acetate (from 0 to 30% ethyl acetate in 53 min). The main fraction was combined and the solvents were removed under reduced pressure, yielding 4-(3,3-dimethylbutanoyl)-2-fluorobenzonitrile (**11a**, 13.80 g, 85%) as a semisolid (pale yellow). ¹H NMR (300 MHz, CDCl₃) δ 1.09 (s, 9H), 2.87 (s, 2H), 7.57−7.93 (m, 3H) ppm. **11a** (1.5 g, 6.84 mmol) was dissolved in MeOH (10 mL). NaBH₄ (0.227 g, 5.99 mmol) was added in small portions (gas evolution). The reaction was stirred for 2 h. The crude was dissolved in ethyl acetate and washed with 1 N HCl, saturated aqueous sodium bicarbonate, and brine. The organic extract was dried over anhydrous sodium sulfate, and the solvent was then removed under reduced pressure. The crude oil was purified by flash chromatography on silica gel (40 g), eluting with mixtures of hexanes/ethyl acetate (from 0 to 70% ethyl acetate in 25 min). The cleanest fractions were combined, and the solvent was removed under reduced pressure, yielding 2-fluoro-4-(1-hydroxy-3,3-dimethylbutyl)benzonitrile (0.433 g, 29%) as a colorless oil. ¹H NMR (300 MHz, CDCl₃) δ 1.05 (s, 9H), 1.53 (dd, J = 14.8, 2.7 Hz, 1H), 1.7 (dd, J = 14.8, 8.9 Hz, 1H), 4.9 (dd, J = 8.8, 2.2 Hz, 1H), 7.2 (m, 2H, obscured by CHCl₃ signal), 7.6 (m, 1H) ppm. 2-Fluoro-4-(1-hydroxy-3,3-dimethylbutyl)benzonitrile (433 mg, 1.9 mmol), and TEA (0.552 mL, 3.96 mmol) were dissolved in dichloromethane (5 mL) at 0 °C. Methanesulfonyl chloride (0.169 mL, 2.18 mmol) was added, and the reaction was stirred for 4 h. The reaction mixture was diluted with dichloromethane, washed with 0.5 N HCl, saturated aqueous sodium bicarbonate, and brine. The organic extract was dried over anhydrous sodium sulfate, and the solvent was removed under reduced pressure, yielding **11b** as an oil which was used in the next step without further purification. ¹H NMR (300 MHz, CDCl₃) δ 1.01 (s, 9H), 1.61 (m, overlap with water, 1H), 2.05 (dd, J = 15.1, 8.85 Hz, 1H), 2.84 (s, 3H), 5.71 (dd, J = 8.85, 3.58 Hz 1H), 7.29 (m, 2H, obscured by CHCl₃ signal), 7.68 (dd, J = 8.10, 6.64 Hz, 1H) ppm.

4-(3,3-Dimethyl-1-((S)-3-(5-methyl-2,4-dioxo-3,4-dihydropyrimidin-1-(2H)-yl)piperidin-1-yl)butyl)-2-fluorobenzonitrile (12). **11b** (4.1 g, 13.70 mmol), (S)-5-methyl-1-(piperidin-3-yl)pyrimidine-2,4-(1H,3H)-dione (**1**, 7.16 g, 34.24 mmol), and DIEA (7.18 mL, 41.09 mmol) were dissolved in acetonitrile (40 mL). The mixture was heated at 70 °C for 20 h. LCMS showed the desired product. The reaction was diluted in ethyl acetate and washed with brine. The organic extract was dried over anhydrous sodium sulfate. After removing the solvent under reduced pressure, the crude was purified by flash chromatography on silica gel (80 g), eluting with mixtures of hexanes/ethyl acetate (from 0 to 100% ethyl acetate in 25 min). The cleanest

fractions were combined, and the solvent was removed under reduced pressure, yielding **12** (0.710 g, 13%) as an off white solid. ^{1}H NMR (300 MHz, CD$_3$OD) δ 0.9 (bs, 9H), 1.56 (bt, 2H), 1.8 (m, 9H), 2.89 (dd, 1H), 2.95 (m, 1H), 3.88 (m, 1H), 4.53 (m, 1H), 7.3 (m, 2H), 7.52 (d, J = 18.6 Hz, 1H), 7.73 (m, 1H) ppm.

2-(3-Bromophenoxy)-4-(3,3-dimethyl-1-((S)-(5-methyl-2,4-dioxo-3,4-dihydropyrimidin-1-(2H)-yl)piperidin-1-yl)butyl)benzoic Acid (13). **12** (2.7 g, 6.55 mmol) was dissolved in NMP (20 mL). 3-Bromophenol (1.699 g, 9.82 mmol) and K$_2$CO$_3$ (2.71 g, 19.64 mmol) were added, and the mixture was split in two and heated in the microwave at 150 °C for 30 min (two vials). The crudes were combined and diluted with ethyl acetate and then washed with aqueous saturated potassium bicarbonate and water. After drying over anhydrous sodium sulfate, the solvent was removed under reduced pressure, yielding a crude oil. The crude was then purified by flash chromatography (220 g) eluting with a mixture of hexanes/ethyl acetate (0−100% in 30 min). The fractions containing product were combined and the solvent removed under reduced pressure, yielding 2-(3-bromophenoxy)-4-(3,3-dimethyl-1-((*S*)-3-(5-methyl-2,4-dioxo-3,4-dihydropyrimidin-1(2*H*)-yl)piperidin-1-yl)butyl)benzonitrile (2.50 g, 67%) as a yellow foam/solid. t_R = 2.58 min, m/z = 565.0, 567.0 (M + 1, M + 3). ^{1}H NMR (300 MHz, CDCl$_3$) δ 0.86 (m, 9H), 1.76 (m, 9H), 2.58 (d, J = 10.9 Hz, 1H), 2.76 (d, J = 10.4 Hz, 1H), 2.8 (m, 1H), 3.64 (m, 1H), 4.56 (m, 1H), 6.76 (m, 1H), 7.03 (m, 2H), 7.17 (m, 1H), 7.31 (m, 2H), 7.66 (dd, J = 7.9, 2.3 Hz, 2H), 9.0 (d, J = 5.1 Hz, 1H) ppm. 2-(3-Bromophenoxy)-4-(3,3-dimethyl-1-((*S*)-3-(5-methyl-2,4-dioxo-3,4-dihydropyrimidin-1(2*H*)-yl)piperidin-1-yl)butyl)-benzonitrile (2.5 g, 4.42 mmol) was then dissolved in ethanol (15 mL) and water (15 mL). Sodium hydroxide (2.65 g, 66.31 mmol) was added, and the mixture was heated at 100 °C for 16 h. The LCMS of the crude showed only acid. The ethanol was removed under a stream of nitrogen. The aqueous solution was treated with concentrated aqueous HCl, and a solid was formed and isolated via filtration. The solid was suspended in ethyl acetate and washed with water. The organic fraction was isolated and dried over anhydrous sodium sulfate, and the solvent was then removed under reduced pressure, yielding the title compound **13** as an off white solid (2 g, 77%). LC-MS (Method 2) t_R = 2.07 min, m/z = 584.1, 586.1 (M + 1, M + 3). ^{1}H NMR (300 MHz, CD$_3$OD) δ 0.85 (s, 9H), 2.01 (m, 9H), 2.36 (br t, 1H), 2.8 (m, 1H), 3.06 (m, 1H), 3.55 (d, J = 11.3 Hz, 1H), 3.73 (d, J = 11.3 Hz, 1H), 4.61 (dd, J = 10.5, 7.9 Hz, 1H), 6.93 (m, 1H), 7.07 (m, 1H), 7.27 (m, 2H), 7.40 (m, 1H), 7.47 (d, J = 4.71 Hz, 1H), 7.60 (d, J = 8.1 Hz, 1H), 8.09 (d, J = 8.1 Hz, 1H) ppm.

2-(3-Bromophenoxy)-4-((R)-3,3-dimethyl-1-((S)-(5-methyl-2,4-dioxo-3,4-dihydropyrimidin-1-(2H)-yl)piperidin-1-yl)butyl)benzoic Acid (14). Diastereomeric mixture **13** was subjected to HPLC preparative chiral separation eluting with a mixture of hexanes (60%), methanol/ethanol (1:1) (40%), and diethylamine (0.5%). The title compound eluted second. After removing the solvent, the sample (825 mg) contained residual diethyl amine that was removed by preparative HPLC (XBridge C18 OBD, 19 mm × 150 mm, 5 μm; flow rate 20 mL/min) eluting with a mixture of a linear gradient from 40 to 69% in 7.5 min methanol in H$_2$O aqueous (0.2% NH$_4$OH). After lyophilizing the sample, the title compound **14** was obtained as an off white solid (400 mg, 15%). LC-MS (Method 2) t_R = 2.2 min, m/z = 584.0, 586.0 (M + 1, M + 3) HRMS calcd for C$_{29}$H$_{35}$BrN$_3$O$_5$ 584.1755, found 584.1746. ^{1}H NMR (300 MHz, CD$_3$OD) δ 0.87 (s, 9H), 1.76 (m, 9H), 2.12 (m, 2H), 2.82 (d, J = 10.7 Hz, 1H), 3.0 (d, J = 7.2 Hz, 1H), 3.84 (t, J = 6.3 Hz, 1H), 4.49 (br s, 1H), 6.9 (m, 2H), 7.04 (d, J = 1.9 Hz, 1H), 7.18 (m, 3H), 7.53 (s, 1H), 7.79 (d, J = 7.91 Hz, 1H) ppm. Diastereomeric ratio: >98:1. Anal. Calcd for C$_{29}$H$_{34}$BrN$_3$O$_5$·H$_2$O·0.05C$_3$H$_8$O: C, 58.51; H, 6.09; N, 6.8. Found: C, 58.41 ; H, 5.92; N, 6.90.

2-(3-Chlorophenoxy)-4-((R)-1-((S)-3-(5-methyl-2,4-dioxo-3,4-dihydropyrimidin-1(2H)-yl)piperidin-1-yl)ethyl)benzoic Acid (35). LC-MS (Method 2) t_R = 1.46 min, m/z = 484.0 (M + 1), 482.2 (M − 1). HRMS calcd for C$_{25}$H$_{27}$ClN$_3$O$_5$ 484.1634, found 484.1618. ^{1}H NMR (300 MHz, CD$_3$OD) δ 1.31 (d, J = 6.03 Hz, 3H), 1.47−1.68 (m, 2H), 1.68−1.86 (m, 5H), 1.99−2.35 (m, 2H), 2.82 (t, J = 10.55 Hz, 2H), 3.61 (d, J = 6.78 Hz, 1H), 4.40 (br s, 1H), 6.73 (d, J = 8.29 Hz, 1H),

6.82 (s, 1H), 6.88−7.05 (m, 2H), 7.19 (t, J = 8.29 Hz, 2 H), 7.49 (s, 1H), 7.78 (d, J = 8.29 Hz, 1H) ppm.

2-(3-Chlorophenoxy)-4-((S)-1-((S)-3-(5-methyl-2,4-dioxo-3,4-dihydropyrimidin-1(2H)-yl)piperidin-1-yl)ethyl)benzoic Acid (36). LC-MS (Method 2) t_R = 1.47 min, m/z = 484.0 (M + 1). HRMS calcd for C$_{25}$H$_{27}$ClN$_3$O$_5$ 484.1634, found 484.1620. ^{1}H NMR (300 MHz, CD$_3$OD) δ 1.30 (d, J = 6.78 Hz, 3H), 1.44−1.83 (m, 7H), 2.08 (d, J = 12.06 Hz, 1H), 2.24 (t, J = 10.17 Hz, 1H), 2.68 (d, J = 12.06 Hz, 1H), 2.96 (d, J = 9.04 Hz, 1H), 3.57 (t, J = 6.40 Hz, 1H), 4.45 (br s, 1H), 6.65−6.86 (m, 2H), 6.87−7.01 (m, 2H), 7.06−7.26 (m, 2H), 7.55 (s, 1H), 7.78 (d, J = 8.29 Hz, 1H) ppm.

(3-Chlorophenoxy)-4-((R)-1-((S)-3-(5-methyl-2,4-dioxo-3,4-dihydropyrimidin-1(2H)-yl)piperidin-1-yl)propyl)benzoic Acid (37). LC-MS (Method 2) t_R = 1.6 min, m/z = 500.0 (M + 1), 496.2 (M − 1). HRMS calcd for C$_{26}$H$_{29}$ClN$_3$O$_5$ 498.1790, found 498.1790. ^{1}H NMR (300 MHz, CD$_3$OD) δ 0.83 (t, J = 7.16 Hz, 3H), 1.88 (s, 3H), 1.93−2.11 (m, 3H), 2.11−2.43 (m, 3H), 2.89 (br s, 1H), 3.09 (br s, 1H), 3.46 (d, J = 10.55 Hz, 1H), 3.56 (br s, 1H), 4.38 (d, J = 7.54 Hz, 1H), 4.68 (br s, 1H), 6.88 (d, J = 8.29 Hz, 1H), 7.00 (s, 1H), 7.13 (d, J = 6.78 Hz, 1H), 7.26 (s, 1 H), 7.34 (t, J = 8.29 Hz, 1H), 7.39−7.56 (m, 2H), 8.09 (d, J = 8.29 Hz, 1H) ppm.

(3-Chlorophenoxy)-4-((S)-1-((S)-3-(5-methyl-2,4-dioxo-3,4-dihydropyrimidin-1(2H)-yl)piperidin-1-yl)propyl)benzoic Acid (38). LC-MS (Method 2) t_R = 1.68 min, m/z = 498.1 (M + 1), 496.2 (M − 1). ^{1}H NMR (300 MHz, CD$_3$OD) δ 0.82 (t, 3H), 1.9 (s and m, 6H), 2.2 (br s, 1H), 3.08 (br s, 1H), 3.48 (br s, 1H), 3.70 (br s, 1H), 4.31 (m, 1H), 4.75 (m overlap with d-solvent signal, 1H), 6.9 (d, 1H), 7.01 (d, 1H), 7.15 (d, 1H), 7.23 (s, 1H), 7.34 (t, 1H), 7.45 (br s, 1H), 8.1 (d, 1H) ppm.

2-(3-Chlorophenoxy)-4-((R)-1-((S)-3-(5-methyl-2,4-dioxo-3,4-dihydropyrimidin-1-(2H)-yl)piperidin-1-yl)butyl)benzoic Acid (39). LC-MS (Method 3) t_R = 1.8 min, m/z = 512.2, 510.1 (M + 1, M − 1). HRMS calcd for C$_{29}$H$_{31}$ClN$_3$O$_5$ 512.1947, found 512.1936. ^{1}H NMR (300 MHz, CD$_3$OD) δ. 0.81 (t, J = 7.16 Hz, 3 H), 0.98−1.30 (m, 2 H), 1.51−1.90 (m, 9 H), 2.11 (t, J = 10.17 Hz, 2 H), 2.70−2.90 (m, 2 H), 3.53 (dd, J = 9.04, 5.27 Hz, 1 H), 4.37 (d, J = 9.04 Hz, 1 H), 6.75 (d, J = 8.29, Hz, 1 H), 6.84 (d, J = 12.81 Hz, 2 H), 6.96 (d, J = 6.03 Hz, 1 H), 7.10 (d, J = 8.29 Hz, 1 H), 7.19 (t, J = 8.29 Hz, 1 H), 7.52 (s, 1 H), 7.77 (d, J = 7.54 Hz, 1 H) ppm. Diastereomeric ratio: >99:1.

2-(3-Chlorophenoxy)-4-((S)-1-((S)-3-(5-methyl-2,4-dioxo-3,4-dihydropyrimidin-1(2H)-yl)piperidin-1-yl)butyl)benzoic Acid (40). LC-MS (Method 2) t_R = 1.86 min, m/z = 512.3 (M + 1), 510.2 (M − 1). HRMS calcd for C$_{27}$H$_{31}$ClN$_3$O$_5$ 512.1947, found 512.1936. ^{1}H NMR (300 MHz, CD$_3$OD) δ 0.81−1.01 (m, 3H), 1.08−1.29 (m, 2H), 1.57−1.97 (m, 9H), 2.12 (t, J = 10.17 Hz, 1H), 2.32 (t, J = 10.17 Hz, 1H), 2.86 (d, J = 11.30 Hz, 1H), 3.07 (d, J = 10.55 Hz, 1H), 3.61 (dd, J = 9.04, 5.27 Hz, 1H), 4.47−4.68 (m, 1H), 6.78−6.96 (m, 2 H), 6.99 (s, 1H), 7.07 (d, J = 7.54 Hz, 1H), 7.16−7.35 (m, 2H), 7.61 (s, 1H), 7.91 (d, J = 8.29 Hz, 1H) ppm. Diastereomeric ratio: >98:1.

2-(3-Chlorophenoxy)-4-((R)-3-methyl-1-((S)-3-(5-methyl-2,4-dioxo-3,4-dihydropyrimidin-1(2H)-yl)piperidin-1-yl)butyl)benzoic Acid (41). LC-MS (Method 2) t_R = 1.9 min, m/z = 526.0 (M + 1). HRMS calcd for C$_{28}$H$_{33}$ClN$_3$O$_5$ 526.2103, found 526.2100. ^{1}H NMR (300 MHz, CD$_3$OD) δ 0.79 (app t, 6H), 1.19 (app t, 1H), 1.31 (m, 1H), 1.66 (m, 6H), 1.75 (s, 3H), 2.11 (d, 2H), 2.86 (m, 3H), 3.64 (m, 1H), 4.38 (m, 1H), 6.75 (dd, 1H), 6.83 (m, 2H), 6.94 (m, 1H), 7.09 (d, 1H), 7.17 (app t, 1H), 7.47 (br s, 1H), 7.71 (d, 1H) ppm.

2-(3-Chlorophenoxy)-4-((S)-3-methyl-1-((S)-3-(5-methyl-2,4-dioxo-3,4-dihydropyrimidin-1(2H)-yl)piperidin-1-yl)butyl)benzoic Acid (42). LC-MS (Method 2) t_R = 1.9 min, m/z = 526.0 (M + 1). HRMS calcd for C$_{28}$H$_{33}$ClN$_3$O$_5$ 526.2103, found 526.2091. ^{1}H NMR (300 MHz, CD$_3$OD) δ 0.76 (app t, 6H), 1.19 (app t, 1H), 1.25 (m, 1H), 1.60 (m, 9H), 1.92 (m, 1H), 2.10 (m, 1H), 2.70 (m, 1H), 2.86 (m, 1H), 3.47 (m, 1H), 4.46 (m, 1H), 6.79 (m, 2H), 6.83 (m, 1H), 6.91 (m, 1H), 7.01 (d, 1H), 7.14 (app t, 1H), 7.49 (br s, 1H), 7.57 (d, 1H) ppm.

2-(3-Bromophenoxy)-4-((S)-3,3-dimethyl-1-((S)-3-(5-methyl-2,4-dioxo-3,4-dihydropyrimidin-1(2H)-yl)piperidin-1-yl)butyl)benzoic Acid (43). LC-MS (Method 2) t_R = 2.0 min, m/z = 586.3 (M + 1), 584.3 (M − 1). HRMS calcd for C$_{29}$H$_{35}$BrN$_3$O$_5$ 584.1755, found

584.1742. ^{1}H NMR (300 MHz, CD$_3$OD) δ 0.75 (s, 9H), 1.47–1.62 (m, 2H), 1.62–1.90 (m, 7H), 1.96 (br s, 1H), 2.16 (t, J = 10.55 Hz, 1H), 2.93 (dd, J = 16.77, 11.68 Hz, 2H), 3.80 (dd, J = 8.29, 3.96 Hz, 1H), 4.48 (br s, 1H), 6.73–6.84 (m, 1H), 6.84–7.00 (m, 2H), 7.02–7.22 (m, 3H), 7.38 (s, 1H), 7.79 (d, J = 7.91 Hz, 1H) ppm. Diastereomeric ratio: >99:1.

2-(3-Chlorophenoxy)-4-((R)-3,3-dimethyl-1-((S)-3-(5-methyl-2,4-dioxo-3,4-dihydropyrimidin-1(2H)-yl)piperidin-1-yl)pentyl)benzoic Acid (44). LC-MS (Method 2) t_R = 2.1 min, m/z = 554.2, 552.2 (M + 1, M + 3). HRMS calcd for C$_{30}$H$_{37}$ClN$_3$O$_5$ 554.2416, found 554.2410. ^{1}H NMR (300 MHz, CD$_3$OD) δ 0.74 (s, 3H), 0.77–0.83 (m, 3 H), 0.85 (s, 3H), 1.16–1.28 (m, 2H), 1.86–2.00 (m, 7H), 2.12 (br s, 1H), 2.24–2.37 (m, 1H), 2.67 (s, 1H), 2.84 (br s, 1H), 3.43–3.64 (m, 3 H), 4.50 (d, J = 11.11 Hz, 1H), 6.88 (dd, J = 8.10, 1.13 Hz, 1H), 6.90–6.94 (m, 1H), 7.12 (d, J = 7.91 Hz, 1H), 7.30–7.38 (m, 2H), 7.42 (s, 1H), 7.52 (d, J = 6.41 Hz, 1H), 8.07 (d, J = 8.10 Hz, 1H) ppm.

2-(3-Chlorophenoxy)-4-((R)-3-ethyl-1-((S)-3-(5-methyl-2,4-dioxo-3,4-dihydropyrimidin-1(2H)-yl)piperidin-1-yl)pentyl)benzoic Acid (45). LC-MS (Method 2) t_R = 2.13 min, m/z = 554.5 (M + 1), 552.5 (M − 1). HRMS calcd for C$_{30}$H$_{37}$ClN$_3$O$_5$ 554.2416, found 554.2415. ^{1}H NMR (300 MHz, CD$_3$OD) δ 0.59–0.82 (m, 6H), 0.93 (br s, 1H), 1.03–1.33 (m, 7H), 1.40–1.79 (m, 9H), 1.94–2.16 (m, 2H), 2.70–2.88 (m, 2H), 2.94 (q, J = 7.28 Hz, 2H), 3.48–3.66 (m, 1H), 4.38 (br s, 1H), 6.67–6.86 (m, 3H), 6.93 (d, J = 7.16 Hz, 1H), 7.06 (d, J = 7.91 Hz, 1H), 7.11–7.25 (m, 1H), 7.47 (s, 1H), 7.68 (d, J = 7.72 Hz, 1H) ppm.

2-(3-Bromophenoxy)-4-((R)-1-((S)-3-(5-methyl-2,4-dioxo-3,4-dihydropyrimidin-1(2H)-yl)piperidin-1-yl)hexyl)benzoic Acid (46). LC-MS (Method 2) t_R = 2.07 min, m/z = 584.2, 586.2 (M + 1, M + 3). HRMS calcd for C$_{29}$H$_{35}$BrN$_3$O$_5$ 584.1755, found 584.1754. ^{1}H NMR (300 MHz, CD$_3$OD) δ 0.70–0.78 (m, 3H), 0.95–1.05 (m, 1H), 1.06–1.21 (m, 5H), 1.56 (d, J = 10.55 Hz, 1H), 1.63–1.84 (m, 7H), 1.98–2.07 (m, 1H), 2.17–2.27 (m, 2H), 2.76 (d, J = 12.06 Hz, 1H), 2.93–2.99 (m, 1H), 3.49 (dd, J = 8.67, 5.65 Hz, 1H), 4.47 (br s, 1H), 6.78–6.83 (m, 1H), 6.87 (d, J = 1.51 Hz, 1H), 6.92–6.95 (m, 1H), 7.09–7.14 (m, 3H), 7.49 (s, 1H), 7.80 (d, J = 8.10 Hz, 1H) ppm.

(2-(3-Bromophenoxy)-4-((R)-3-ethyl-3-methyl-1-((S)-3-(5-methyl-2,4-dioxo-3,4-dihydropyrimidin-1(2H)-yl)piperidin-1-yl)pentyl)-benzoic Acid (47). LC-MS (Method 2) t_R = 2.26 min, m/z = 612.1, 614.1 (M + 1, M + 3). HRMS calcd for C$_{31}$H$_{39}$BrN$_3$O$_5$ 612.2068, found 612.2075. ^{1}H NMR (300 MHz, CD$_3$OD) δ 0.69–0.81 (m, 9 H), 1.13–1.34 (m, 4H), 1.61 (d, J = 8.67 Hz, 2H), 1.74–1.89 (m, 7H), 1.90–2.00 (m, 1H), 2.17 (t, J = 10.46 Hz, 1H), 2.94 (br s, 2H), 3.76 (t, J = 6.03 Hz, 1H), 4.58 (br s, 1H), 6.83–6.99 (m, 2H), 7.03–7.10 (m, 1H), 7.14–7.26 (m, 3H), 7.54 (s, 1H), 7.81 (d, J = 7.91 Hz, 1H) ppm.

2-(3-Chlorophenoxy)-4-((R)-3,3-dimethyl-1-((S)-3-(5-methyl-2,4-dioxo-3,4-dihydropyrimidin-1(2H)-yl)piperidin-1-yl)hexyl)benzoic Acid (48). LC-MS (Method 2) t_R = 2.16 min, m/z = 568.1 (M + 1), 566.2 (M − 1). HRMS calcd for C$_{31}$H$_{39}$ClN$_3$O$_5$ 568.2573, found 568.2562. ^{1}H NMR (300 MHz, CD$_3$OD) δ 0.64 (s, 3H), 0.69 (t, J = 6.78 Hz, 3H), 0.75 (s, 3H), 0.92–1.20 (m, 4H), 1.72–1.91 (m, 7H), 2.02 (d, J = 9.23 Hz, 1 H), 2.18–2.31 (m, 1H), 2.60 (br s, 1H), 2.85 (br s, 1H), 3.44 (d, J = 7.72 Hz, 1H), 3.52 (d, J = 10.74 Hz, 1H), 4.45 (d, J = 10.55 Hz, 1H), 4.55 (d, J = 7.54 Hz, 1H), 6.77 (ddd, J = 8.29, 2.45, 0.75 Hz, 1H), 6.80–6.84 (m, 1H), 7.01 (ddd, J = 8.01, 1.88, 0.85 Hz, 1H), 7.18–7.26 (m, 2 H), 7.29 (d, J = 1.13 Hz, 1H), 7.44 (dd, J = 8.01, 1.60 Hz, 1H), 7.97 (d, J = 8.10 Hz, 1H) ppm. Diastereomeric ratio: >99:1

2-(3-Chlorophenoxy)-4-((R)-2-cyclohexyl-1-((S)-3-(5-methyl-2,4-dioxo-3,4-dihydropyrimidin-1(2H)-yl)piperidin-1-yl)ethyl)benzoic Acid (49). LC-MS (Method 1) t_R = 2.12 min, m/z = 566.3 (M + 1), 564.3 (M − 1). HRMS calcd for C$_{31}$H$_{37}$ClN$_3$O$_5$ 566.2416, found 566.2412. ^{1}H NMR (300 MHz, CD$_3$OD) δ 0.70–0.93 (m, 3H), 1.03 (d, J = 7.72 Hz, 4H), 1.19 (t, J = 7.35 Hz, 4H), 1.36–1.70 (m, 10H), 1.70–1.81 (m, 3H), 1.88–2.15 (m, 2H), 2.78 (dd, J = 17.43, 11.77 Hz, 2H), 2.94 (q, J = 7.41 Hz, 2H), 3.57 (dd, J = 9.42, 5.84 Hz, 1H), 4.37 (br s, 1H), 6.70–6.86 (m, 3H), 6.92 (dd, J = 8.01, 1.04 Hz, 1H), 6.97–7.07 (m, 1H), 7.07–7.22 (m, 1H), 7.45 (s, 1H), 7.59 (d, J = 7.91 Hz, 1H) ppm.

2-(3-Chlorophenoxy)-4-((R)-1-((S)-3-(5-methyl-2,4-dioxo-3,4-dihydropyrimidin-1(2H)-yl)piperidin-1-yl)-2-(tetrahydro-2H-pyran-4-yl)ethyl)benzoic Acid (50). LC-MS (Method 2) t_R = 1.60 min, m/z = 568.2 (M + 1), 566.3 (M − 1). HRMS calcd for C$_{30}$H$_{35}$ClN$_3$O$_6$ 568.2209, found 568.2203. ^{1}H NMR (300 MHz, CD$_3$OD) δ 1.08–1.33 (m, 3H), 1.41 (d, J = 12.62 Hz, 1H), 1.55 (d, J = 11.11 Hz, 3H), 1.61 (br s, 1H), 1.65–1.83 (m, 6H), 1.83–1.99 (m, 1H), 2.14 (t, J = 10.27 Hz, 1H), 2.76 (d, J = 10.93 Hz, 1H), 2.90 (d, J = 9.98 Hz, 1H), 3.55–3.68 (m, 1H), 3.76 (d, J = 11.87 Hz, 2H), 4.45 (br s, 1H), 6.69–6.81 (m, 2H), 6.86 (s, 1H), 6.89–7.01 (m, 1H), 7.06–7.28 (m, 2 H), 7.44 (s, 1H), 7.79 (d, J = 7.91 Hz, 1H) ppm. Diastereomeric ratio: >99:1.

(2-(3-Bromophenoxy)-4-(R)-(2-(1-adamantane)-1-((S)-3-(5-methyl-2,4-dioxo-3,4-dihydropyrimidin-1(2H)-yl)piperidin-1-yl)ethyl)-benzoic Acid (51). LC-MS (Method 2) t_R = 2.45 min, m/z = 662, 664 (M + 1, M + 3). HRMS calcd for C$_{35}$H$_{41}$BrN$_3$O$_5$ 662.2224, found 662.2230. ^{1}H NMR (300 MHz, DMSO-d_6) δ 1.1–1.8 (m, 25H), 2.62 (d, 1H), 2.78 (m, 1H), 3.69 (m, 2H), 4.26 (m, 1H), 6.63 (s, 1H), 6.72 (m, 2H), 6.90 (d, 1H), 6.97 (d, 1H), 7.18 (t, 2H), 7.39 (d, 1H), 7.52 (s, 1H) ppm. Diastereomeric ratio: 99:1.

■ ASSOCIATED CONTENT

Ⓢ Supporting Information

Enzymatic, MIC, and log *D* assay protocols as well as protein crystallography methods and statistics tables. This material is available free of charge via the Internet at http://pubs.acs.org. PDB accession codes: 4HEJ (compound (*S*)-**16**); 4GSY (**34**); 4HDC (**41**).

■ AUTHOR INFORMATION

Corresponding Author
*E-mail: gabriel@sagerx.com. Phone: +1.617.299.8375.

Present Address
‖Sage Therapeutics, 215 First Street, Cambridge, MA 02141, United States.

Notes
The authors declare no competing financial interest.

■ ACKNOWLEDGMENTS

■ ABBREVIATIONS

TMK, thymidylate kinase; Spn, *Streptococcus pneumoniae*; Sau, *Staphylococcus aureus*; MIC, minimum inhibitory concentration

■ REFERENCES

(1) Silver, L. L. Challenges of Antibacterial Discovery. *Clin. Microbiol. Rev.* **2011**, *24*, 71−109.

(2) (a) Payne, D. J.; Gwynn, M. N.; Holmes, D. J.; Pompliano, D. Drugs for Bad Bugs: Confronting the Challenges of Antibacterial Discovery. *Nat. Rev. Drug Discovery* **2007**, *6*, 29−40. (b) Barrett, J. F. Impact of Genomics-Emerging Targets for Antibacterial Therapy. *Comprehensive Med. Chem. II* **2006**, *7*, 731−748.

(3) Fischbach, M. A.; Walsh, C. T. Antibiotics for Emerging Pathogens. *Science* **2009**, *325*, 1089−1093.

(4) Charifson, P. S.; Grossman, T. H.; Mueller, P. The Use of Structure-Guided Design to Discover New Anti-Microbial Agents:

Focus on Antibacterial Resistance. *Anti-Infect. Agents Med. Chem.* **2009**, 8, 73−86.

(5) Schneider, P.; Hawser, S.; Islam, K. Iclaprim, a Novel Diaminopyrimidine with Potent Activity on Trimethoprim Sensitive and Resistant Bacteria. *Bioorg. Med. Chem. Lett.* **2003**, 13, 4217−4221.

(6) (a) Charifson, P. S.; Anne-Laure Grillot, A.-L.; Grossman, T. H.; Parsons, J. D.; Badia, M.; Bellon, S.; Deininger, D. D.; Drumm, J. E.; Gross, C. H.; LeTiran, A.; Liao, Y.; Mani, N.; Nicolau, D. P.; Perola, E.; Ronkin, S.; Shannon, D.; Swenson, L. L.; Tang, Q.; Tessier, P. R.; Tian, S.-K.; Trudeau, M.; Wang, T.; Wei, Y.; Zhang, H.; Stamos, D. Novel Dual-Targeting Benzimidazole Urea Inhibitors of DNA Gyrase and Topoisomerase IV Possessing Potent Antibacterial Activity: Intelligent Design and Evolution through the Judicious Use of Structure-Guided Design and Stucture−Activity Relationships. *J. Med. Chem.* **2008**, 51, 5243−5263. (b) Eakin, A. E.; Green, O.; Hales, N.; Walkup, G. K.; Bist, S.; Singh, A.; Mullen, G.; Bryant, J.; Embrey, K.; Gao, N.; Breeze, A.; Timms, D.; Andrews, B.; Uria-Nickelsen, M.; Demeritt, J.; Loch, J. T., III; Hull, K.; Blodgett, A.; Illingworth, R. N.; Prince, B.; Boriack-Sjodin, P. A.; Hauck, S.; MacPherson, L. J.; Ni, H.; Sherer, B. Pyrrolamide DNA gyrase inhibitors: fragment-based nuclear magnetic resonance screening to identify antibacterial agents. *Antimicrob. Agents Chemother.* **2012**, 56, 1240−1246.

(7) Keating, T. A.; Newman, J. V.; Olivier, N. B.; Otterson, L. G.; Andrews, B.; Boriack-Sjodin, P. A.; Breen, J. N.; Doig, P.; Dumas, J.; Gangl, E.; Green, O. M.; Guler, S. Y.; Hentemann, M. F.; Joseph-McCarthy, D.; Kawatkar, S.; Kutschke, A.; Loch, J. T.; McKenzie, A. R.; Pradeepan, S.; Prasad, S.; Martínez-Botella, G. *In Vivo* Validation of Thymidylate Kinase (TMK) with a Rationally-Designed, Selective Antibacterial Compound. *ACS Chem. Biol.* DOI: 10.1021/cb300316n. Published online: Aug 21, **2012**.

(8) (a) Vanheusden, V.; Van Rompaey, P.; Munier-Lehmann, H.; Pochet, S.; Herdewijn, P.; Van Calenbergh, S. Thymidine and thymidine-5′-O-monophosphate analogues as inhibitors of *Mycobacterium tuberculosis* thymidylate kinase. *Bioorg. Med. Chem. Lett.* **2003**, 13, 3045−3048. (b) Choi, J. Y.; Plummer, M. S.; Starr, J.; Desbonnet, C. R.; Soutter, H.; Chang, J.; Miller, J. R.; Dillman, K.; Miller, A. A.; Roush, W. R. Structure Guided Development of Novel Thymidine Mimetics Targeting *Pseudomonas aeruginosa* Thymidylate Kinase: From Hit to Lead Generation. *J. Med. Chem.* **2012**, 55, 852−870.

(9) Kotaka, M.; Dhaliwal, B.; Ren, J.; Nichols, C. E.; Angell, R.; Lockyer, M.; Hawkins, A. R.; Stammers, D. K. Structures of *S. aureus* thymidylate kinase reveal an atypical active site configuration and an intermediate conformational state upon substrate binding. *Protein Sci.* **2006**, 15, 774−784.

(10) Martínez-Botella, G.; Breen, J. N.; Duffy, J. E. S.; Dumas, J.; Geng, B.; Gowers, I. K.; Green, O. M.; Guler, S.; Hentemann, M. F.; Hernandez-Juan, F. A.; Joseph-McCarthy, D.; Kawatkar, S.; Larsen, N. A.; Lazari, O.; Loch, J. T.; Macritchie, J. A.; McKenzie, A. R.; Newman, J. V.; Olivier, N. B.; Otterson, L. G.; Owens, A. P.; Read, J.; Sheppard, D. W.; Keating, T. A. Unpublished results.

(11) Topliss, J. G. Utilization of Operational Schemes for Analog Synthesis in Drug Design. *J. Med. Chem.* **1972**, 15, 1006−1011.

(12) Fersht, A. R.; Shi, J.-P.; Knill-Jones, J.; Lowe, D. M.; Wilkinson, A. J.; Blow, D. M.; Brick, P.; Carter, P.; Waye, M. M. Y.; Winter, G. Hydrogen bonding and biological specificity analysed by protein engineering. *Nature* **1985**, 314, 235−238.

(13) (a) Friesner, R. A.; Banks, J. L.; Murphy, R. B.; Halgren, T. A.; Klicic, J. J.; Mainz, D. T.; Repasky, M. P.; Knoll, E. H.; Shelley, M.; Perry, J. K.; Shaw, D. E.; Francis, P.; Shenkin, P. S. Glide: a new approach for rapid, accurate docking and scoring. 1. Method and assessment of docking accuracy. *J. Med. Chem.* **2004**, 47, 1739−1749. (b) Halgren, T. A.; Murphy, R. B.; Friesner, R. A.; Beard, H. S.; Frye, L. L.; Pollard, W. T.; Banks, J. L. Glide: a new approach for rapid, accurate docking and scoring. 2. Enrichment factors in database screening. *J. Med. Chem.* **2004**, 47, 1750−1759.

(14) Kaminski, G. A; Friesner, R. A.; Tirado-Rives, J.; Jorgensen, W. L. Evaluation and Reparametrization of the OPLS-AA Force Field for Proteins via Comparison with Accurate Quantum Chemical Calculations on Peptides. *J. Phys. Chem. B* **2001**, S, 6474−6487.

(15) (a) Bieber, P. *Comptes Rendus* **1951**, 233, 655. (b) Csuk, R.; von Scholz, Y. Synthesis of racemic carbocyclic cyclopropanoid nucleoside analogues. *Tetrahedron* **1995**, 51 (26), 7193. (c) Kovačková, S.; Dračínský, M.; Rejman, D. The synthesis of piperidine nucleoside analogs - a comparison of several methods to access the introduction of nucleobases. *Tetrahedron* **2011**, 67, 1485−1500.

■ NOTE ADDED AFTER ASAP PUBLICATION

After this paper was published online October 24, 2012, reference 15c was added to the reference list. The corrected version was reposted November 7, 2012.